A.4 Propulsion

A.4.1 Introduction

The propulsion system is a large and important subsystem in any launch vehicle. The overall goal of the propulsion group is to provide a comprehensive feasibility analysis of the obstacles associated with inexpensively propelling a payload into low Earth orbit. Over the course of the semester, we research many different topics and create models for a variety of tasks.

We start by analyzing the many different launch methods that could potentially aid the design team in reducing costs. Then we research a variety of propellants and propellant combinations, as well as the hardware necessary to turn those propellants into a motive force. At the same time, we create sizing codes for determining propellant and engine masses. We choose a handful of the most promising propellant combinations for use in the model analysis (see section A.7).

We also perform more detailed research and analysis on various components: injectors, nozzles, pressurization systems, attitude control systems, and engine performance.

The following pages provide details on the propulsion groups' work.

A.4.2 Design Methods

A.4.2.1 Launch Method Analysis

A.4.2.1.1 Ground Launch

For the ground launch, we consider the different configurations that we can use to launch a payload into orbit using a standard rocket. We look at staging, engine types, fuel types, attitude control, pressurization systems, nozzles, etc.

The first step in the design is the determination of the number of stages we will be using. After testing various propulsion codes we developed, we show that using two to three stages is the best option for a ground launch. Using this number of stages reduce the total mass that is needed in terms of inert mass of the rocket and fuel. Using more than three stages does not have the same savings in terms of mass and cost. So, we only consider using two to three stages.

The next part of our design involves looking at the various types of engines types, fuels, and other propulsion considerations. These are covered with much more depth in the following sections of the appendix.

A.4.2.1.2 Air Launches

An air launch system includes a carrier vehicle as well as a launch vehicle. The carrier vehicle may be either a balloon or an aircraft and is used to take the launch vehicle to a higher altitude where the launch vehicle is released and ignited to reach orbit. In order to determine the feasibility of air launch vehicles, we must first look at the benefits and disadvantages in comparison with a conventional ground launch. A comparison of the Δv benefits, ease of implementation and key features of each air launch method is studied in order to get an overview of their respective strengths and weaknesses.

In order to reach Low Earth Orbit (LEO), a spacecraft must attain a velocity change (Δv) of approximately 8000m/s. A lower change in velocity is a large advantage since it lowers the amount of propellant needed which lowers the total weight of the rocket and in turn lowers the cost of the total launch system. There are several losses present in a launch. The key losses due to launch altitude are atmospheric, gravitational and pressure drag losses.

Atmospheric and gravitational drag of a launch from the ground typically adds 1,500 to 2,000m/s to the Δv requirement. Furthermore, because drag losses are subjected to the "cubed-squared" law, decreasing the launch vehicle size will increase the drag losses.[1] The drag loss of the launch vehicle can be reduced by launching at an altitude after a boost from a carrier vehicle, either a balloon or an aircraft.

Gravitational losses are losses incurred due to the rocket's work against the Earth's gravitational pull. These losses are highly dependent on the thrust to weight ratio (T/W) of the rocket and are approximately 1,150 to 1,600m/s for a ground launched vehicle depending on the size of the vehicle. The gravitational losses of a launch can also be reduced by an air launch due to the higher altitude of launch. This allows the vehicle to turn horizontal earlier to minimize gravitational losses.[1]

Atmospheric pressure loss is due to the dependence of the performance of a rocket motor on the atmospheric pressure. A rocket motor works best in a vacuum. Air launching will always reduce

the atmospheric pressure loss due to the lower ambient pressure at altitude as compared to sea level. The losses for our vehicles can be found in the Sections 4.1.2, 4.2.2 and 4.3.2.

For a launch from a carrier aircraft, the aircraft speed will directly reduce the Δv required to attain LEO. However, the majority of the Δv benefits from an air launch results from the angle of attack of the vehicle during the release of the rocket. The ideal angle is somewhere between 25° to 30°.[1]

A study by Klijn et al. concluded that at an altitude of 15,250 m, a rocket launch with the carrier vehicle having a zero launch velocity at an angle of attack of 0° to the horizontal experienced a Δv benefit of approximately 600m/s while a launch at a velocity of 340m/s at the same altitude and angle of attack resulted in a Δv benefit of approximately 900m/s. The zero launch velocity situations can be used to represent the launch from a balloon as it has no horizontal velocity.

Furthermore, by increasing the angle of attack of the carrier vehicle to 30° and launching at 340m/s, they obtained a Δv gain of approximately 1,100m/s. Increasing the launch velocity to 681m/s and 1,021m/s produced a Δv gain of 1,600m/s and 2,000m/s respectively.

From this comparison, it can be seen that in terms of the Δv gain, an air launch is superior to a ground launch. As the size of the vehicle decreases, this superiority will have a larger effect due to the increased effective drag on the vehicle.

One of the main benefits of an aircraft launch is the fact that an aircraft can fly to an advantageous location to avoid adverse weather conditions that ground launches cannot escape. This advantage is especially useful if the launch is needed on demand. Also, since the launch vehicle is launched from the air, no equipment, such as a launch pad, or on-site requirements, are needed.

A disadvantage in using an aircraft launch system would be the cost of obtaining an aircraft for use. Purchasing an aircraft is a large investment ranging from thousands to millions of dollars. Leasing an aircraft is an affordable alternative to purchasing, but the selection and availability of

an aircraft lease is very narrow. Another disadvantage is that the aircraft usually has to be modified in order to accommodate the launch vehicle. When looking at pre-existing aircraft, a vehicle that has flown with a rocket or a missile underneath is advantageous because they already have the necessary modifications. These aircraft vehicles can be leased or purchased with little additional modification cost.

There are various methods of attaching the launch vehicle to the carrier aircraft. Two such methods are the captive on bottom and internally carried methods. [2]

The captive on bottom method has the advantage of proven and easy separation from the carrier aircraft. The main disadvantage of this method is that there are limits to the launch vehicle size due to aircraft clearance limitations. However, in the case of small payloads, it would be possible to design the launch vehicle within the confines of an existing attachment such as a missile. The disadvantage of this is that commercial aircraft are almost never designed to carry missiles and would require modifications, increasing the developmental cost. An alternative would be to use a military jet such as the F-15 and design within the constraints of an existing missile. We know that the F-15 is easily capable of hauling the 231kg AIM-7 Sparrow air-to-air missile. We also know that the F-15 has launched an anti-satellite (ASAT) missile weighing 1180kg flying at Mach 1.22 at an altitude of 11.6km and an angle of attack of 65 degrees. [2]

Another captive on bottom method would be to use the White Knight aircraft that carried SpaceShipOne to launch altitude. The White Knight is commercially available and would be easier to procure and license in comparison with a military aircraft. However, the launch velocity of the White Knight will be far lower than that of an F-15.

An internally carried launch vehicle would be one such as the Pegasus launch system. A plane would have to be redesigned in order to accommodate a launch vehicle. Cargo planes can be used due to their high payload capacities. The disadvantage of this method is that steering losses will be incurred in order to accelerate the launch vehicle and bring it into a climb to exit the atmosphere. Furthermore, the velocity of a cargo plane would be limited to subsonic velocities in the range of what the White Knight attains.

A significant disadvantage of air launch vehicles is due to propellant boil off. Propellant boil off is already an occurring problem for cryogenic propellants. When you combine cryogenic propellants with an air launch system, propellant boil off becomes an even greater problem. In the case of the X-15, a rocket launched off of a B-52, during its 45-60 minute climb attached to the aircraft 60% to 80% of its liquid oxygen boiled off, due to additional heating from the sun and the air flow.[1]

Safety is still a large issue with air launch vehicles. Many problems may arise that could cause harm to the aircraft, crew, and innocent victims. Since air launches are still not widely used, like ground launches, there are probably more problems that will arise until the processes and procedures mature. Problems can range from the ignition not starting, in the case of the X-15, to igniting before being released from the aircraft.[1]

A balloon launch would require either the design of a new balloon or possibly using existing weather balloons. However, existing designs aren't usually designed to support the weight required for a launch vehicle. Purposefully designed balloons such as the NASA's Ultra-High Altitude Balloon (UHAB) vehicles are able to carry payloads of 900-1,000 kg to an altitude of 45 km. However, unless the balloon was designed to sustain the environment of launch, it will likely be damaged and be a once off carrier vehicle. Designing the balloon to be tougher would increase the developmental cost while using existing designs would increase the per launch cost.[3] For a disposable balloon, it would be possible to simply fire the launch vehicle through the balloon. This has been previously used by the US Navy in the 1950s in the form of the Rockoon. However, as of yet, there has never been an orbital flight that has been successfully launched from a balloon.

Looking at the complexities of aircraft launches, the simplest method of obtaining the benefits of an air launch would be to design a simple balloon equipped with a simple gondola which the launch vehicle would then fire out of, straight through the balloon. This would mitigate the costs of development, maintenance and recovery.

References

[1] Sarigul-Klijn, N., et al. "Air Launching Earth-to-Orbit Vehicles: Delta V gains from Launch Conditions and Vehicle Aerodynamics," AIAA Paper 2004-872, Jan 2004.

[2] Sarigul-Klijn, N., et al. "A Study of Air Launch Methods for RLVs," AIAA Paper 2001-4619, August 2001.

[3] Gizinski, J., et al. "Small Satellite Delivery Using a Balloon-Based Launch System," AIAA Paper 92-1845, March 1992.

A.4.2.1.2.1 Aircraft

We now look at a few aircrafts to research their feasibility for our mission requirements. We look at both military and commercial aircraft to exemplify the unique advantages each brings to a launch system. The main focuses of the aircraft research are the amount of modification that is already made, the cost of leasing and/or purchasing aircraft, and the performance benefits the aircraft can give to a launch vehicle.

The F-15 is a military aircraft that has been in use since 1989 and will continue to be in service until 2025. Currently, the F-15 launches various missiles captive on bottom and releases them at top speeds. An existing launch vehicle used with the F-15 carrier aircraft is the ASM-135 AST anti-satellite weapon. The modifications made to the F-15 to carry the launch vehicle allow for a vehicle 3.66 meter length by 0.53 meter span and a payload weight of 1,180 kg.[1] The F-15 is capable of carrying a larger launch vehicle but more modifications would need to be made to fit the larger size. The F-15 is exclusively sold to the military, so the only way of being able to lease this aircraft to launch a vehicle would be through the government. The government unfortunately does not lease out any of their aircraft. The cost of purchasing an F-15 from the Boeing Company is estimated at $42,520,000.[1] Also, if an aircraft is purchased, there are additional costs of operations and maintenance added to the overall price. The price of the aircraft and small launch vehicle area eliminates the F-15 as an option for use in our air launch system.

The L-1011 Stargazer is a Lockheed Martin aircraft that has been converted into a launch vehicle carrier by Orbital Sciences for their Pegasus program. The Pegasus program is very similar to the type of air launch system that our project entails. The Stargazer brings the Pegasus launch vehicle to an altitude of 11,890 m where it is then released and ignites to orbit.[2] The aircraft is capable of carrying a 17.1 meter length by 7.9 meter span rocket with a weight of 36,800 kg.[2] The Stargazer is a one of a kind aircraft that would have to be leased exclusively from Orbital Sciences. Unfortunately, no one could be reached to determine the cost for leasing this aircraft for use in our project. The purchase price for an unmodified L-1011 is estimated at $30 million.[2] Again, like the F-15, operations and maintenance is not included in the purchase cost. Due to the larger payload area and lower purchase price, the L-1011 Stargazer is a potential aircraft carrier for our launch vehicle but research for the White Knight is needed for comparison.

Author: Stephanie Morris, William Yeong Liang Ling

The White Knight is the aircraft used by Scaled Composites to launch the Ansari X-Prize winner SpaceShipOne. This was a private competition to send a reusable manned vehicle to suborbital space and back. The White Knight was created with a low-cost mission in mind so it seems feasible that this aircraft would be a competitive choice for our low-cost launch system. The White Knight carries SpaceShipOne to an altitude of 15,000 meters where it is then released with an initial velocity of 59.72 m/s and continues to climb to the limits of space.[3] White Knight allows for a launch vehicle to fill an 8.2 meter length by 8.2 meter span with a payload of 3,629 kg.[3] The representatives from Scaled Composites were very helpful in giving accurate estimates specific to our project. The cost for leasing the White Knight is $5,030/hr which includes crew time, fuel and flight time.[4] This rate is feasible for a low cost launch system such as ours.

Overall, the White Knight can be a solution to our low cost launch system by bringing our launch vehicle to a higher altitude with an initial velocity. The performance characteristics and cost modifiers are included in the optimization code for our overall design.

References

[1]Wade, M., "F-15," *Encyclopedia Astronautica*. [http://www.astronautix.com/stages/f15.htm. Accessed 1/19/08-1/23/08.]

[2] Wade, M., "Lockheed L-1011," *Encyclopedia Astronautica*. [http://www.astronautix.com/stages/l1011.htm. Accessed 1/19/08-1/23/08.]

[3]Scaled Composites, "Tier One – Private Manned Space Program," Scaled Composites LLC. [http://www.scaled.com/projects/tierone. Accessed 1/19/08-1/23/08.]

[4]Williams, Bob, Sales representative of Scaled Composites. "Email Conversation," Dates 1/22/08 through 1/31/08.

A.4.2.1.2.2 Balloon

Our balloon launch platform design goes through three phases. The first phase is a historical model. The second phase involves the creation of our own physical model. Lastly, we refine the balloon and the gondola.

First, we modeled the balloon after a feasibility study done by Gizinski and Wanagas.[1] The mass and breakdown of their balloon design is seen below in Tables A.4.2.1.3.1 and A.4.2.1.3.2.

Table A.4.2.1.3.1 Mass of Gondola Elements[1]

Gondola Elements	Mass (lbm)
Cardboard Sections	100
ACS	100
Telemetry System	30
Flight Support Computer	50
Batteries	100
Steel Cables	70
Framework, Mechanisms	1050
Chute System	150
Electrical Cables	100
Swivel	50

Table A.4.2.1.3.2 Mass of Rocket Elements[1]

Rocket Elements	Mass (lbm)
Engine Tank Structure	650
Avionics	100
Payload	250
Payload Fairing	100
Cabling	50
Propellant	6800
Attitude Control	50
Total	8000

We scale these masses by a payload ratio between the desired payload and the payload given in Table A.4.2.1.3.2.

Breaking away from the historical model, we derive a mathematical model of our own balloon. We begin by using a free body diagram. This diagram is seen in Fig. A.4.2.1.3.1.

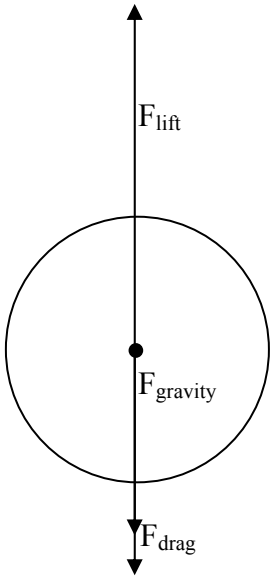

Fig.A.4.2.1.3.1: Vertical free body diagram of the balloon.
(William Ling)

We will first consider stationary motion where the drag force, F_{drag}, is zero. There are two other forces acting on the balloon platform, lift (F_{lift}) and weight ($F_{gravity}$). The lift force is found using the method outlined in the document by Tangren.[2] The buoyancy force is defined as the difference between the lift and weight in this case.

Our final goal is for the code to input a desired rocket mass and final altitude in order to output the size of the balloon. Using Archimedes' principle, the static lift of the balloon can be determined by considering the displaced volume of air by the lifting gas. This can be expressed as a lift coefficient to determine the lifting force of the gas.

$$C_l = \rho_a - \rho_g \qquad \text{(A.4.2.1.2.2.1)}$$

where C_l is the lift coefficient of the lifting gas, ρ_a is the density of air and ρ_g is the density of the lifting gas where all three terms are in units of kg/m^3. It must be noted that this lift

coefficient is a calculation tool and not analogous to an aircraft's lift coefficient which is dimensionless.

To determine the lift coefficient of the lifting gas at a desired altitude, we must take into account the combined gas law determined by the combination of the Law of Charles and Gay-Lussac (1802) and Boyle's Law (1662).

$$\frac{P_0 V_0}{T_0} = \frac{PV}{T} \tag{A.4.2.1.2.2.2}$$

where P_0, V_0 and T_0 are the pressure, volume, and temperature at an initial condition which will be set at the standard sea level (SSL) while P, V and T are the same values at a final condition, i.e. at the desired altitude.

The volume of a gas has a direct and inverse relation to its density. By substituting the density, ρ, of the gas for the volume V into Eq. (A.4.2.1.2.2.2) and solving for ρ, we then obtain

$$\rho = \frac{P}{P_0}\frac{T_0}{T}\rho_0 \tag{A.4.2.1.2.2.3}$$

where all terms are as previously defined and the initial condition will be set at SSL.

By assuming that the fractional densities provided by the standard atmosphere applies to all other gases, the use of the ρ/ρ_0 ratio in Eq. (A.4.2.1.2.2.1) will allow the determination of the lift coefficient at a desired altitude based on SSL conditions.[2]

$$C_{l,s} = \left(\frac{\rho}{\rho_0}\right) C_{l,0} \tag{A.4.2.1.2.2.4}$$

where $C_{l,s}$ is the lift coefficient at a desired altitude, $C_{l,0}$ is the lift coefficient at SSL as determined by Eq. (A.4.2.1.2.2.1) using SSL conditions, ρ is the density of the air at the desired

altitude based on the standard atmosphere and ρ_0 is the density of the air at SSL. The units of all terms in Eq. (A.4.2.1.2.2.4) are kg/m^3.

The assumptions we make in this derivation are that the temperature and pressure inside the balloon are identical to that of the out air and that all gases involved are perfect gases. Furthermore, we are also assuming the standard atmosphere to be accurate.

To account for the diffusion of air into the balloon and gas out of the balloon, the standard practice is to assume a 95% gas purity.[2] Furthermore, for stable flight of the balloon, especially during strong winds, experience by others has shown that the gross static lift should exceed the load of the balloon by 15%.[2] The actual lift coefficient is then,

$$C_l = 0.95 \times 0.85 \times \left(\frac{\rho}{\rho_0}\right) C_{l,0}$$
$$C_l = 0.8075 \left(\frac{\rho}{\rho_0}\right) C_{l,0} \quad \text{(A.4.2.1.2.2.5)}$$

This term allows us to determine the lift of a unit volume of lifting gas at a specified altitude. The volume of the balloon required can then be determined by dividing the static lift in kg by the lift coefficient.

We make the assumption that the required static thrust of the balloon will be equal to the total mass of the balloon including all attachments such as the launch vehicle, the gondola, instruments and tethers at the desired altitude. This assumption would mean that the balloon would rise from the ground and stabilize over time at the desired altitude by oscillating up and down. Another assumption is that the balloon will take the shape of a perfect sphere at all times. In reality, the balloon will start as an ice-cream shape with the lifting gas above the cone. As the gas expands, the sphere above the cone would expand while the size of the cone would reduce, eventually resulting in a single sphere. The following are the masses of our balloon and accompanying payloads,

Table A.4.2.1.2.2.1 Mass breakdown of the balloon and payloads

Variable	Value	Units
$M_{balloon}$	$\pi d^2 \times \rho_{material} \times t_{material}$	kg
$M_{gondola}$	Variable, depending on payload[a]	kg
M_{rocket}	Variable, specified input	kg

[a] 177.188 kg, 227.114 kg and 338.32 kg for the 200 g, 1 kg and 5 kg payloads respectively.

where d is the diameter of the balloon, $\rho_{material}$ is the density of the balloon material in kg/m^3 and $t_{material}$ is the thickness of the balloon material. We make another assumption that the thickness of the balloon material is thin enough for the volume to be approximated with a simple volume equation. The total mass without the lifting gas is therefore,

$$M_{total} = M_{balloon} + M_{gondola} + M_{rocket}$$
$$M_{total} = \pi d^2 \rho_{material} t_{material} + M_{gondola} + M_{rocket} \quad \text{(A.4.2.1.2.2.6)}$$

The required lifting gas volume must be contained within a sphere of diameter d. This is also equal to the total mass divided by the lift coefficient.

$$V = \frac{\pi}{6} d^3 = \frac{M_{total}}{C_l} \quad \text{(A.4.2.1.2.2.7)}$$

By substituting Eq. (A.4.2.1.2.2.6) into Eq. (A.4.2.1.2.2.7) and rearranging, we then obtain,

$$(C_l \frac{\pi}{6}) d^3 - (\pi \rho_{material} t_{material}) d^2 - M_{gondola} - M_{rocket} = 0 \quad \text{(A.4.2.1.2.2.8)}$$

This is a cubic equation and hence, as can be expected, the diameter d will always have a real solution. The diameter can then be substituted back into Eq. (A.4.2.1.2.2.7) to determine the required lifting gas volume.

The next step in our design is the refinement of our preliminary design. First, we must choose the gas used in the balloon. The two gases to consider are helium and hydrogen. Hydrogen costs less than helium and is half the density of helium. Helium, however, is much more stable. After

looking at the cost benefits and the safety concerns raised by using hydrogen as a lifting gas, helium is chosen as our lifting gas.

We now consider alternative designs for the balloon. We initially assume the balloon to be a perfect sphere. At this stage, we must also consider alternatives to a single balloon by studying the purpose of the balloon. Firstly, we want to launch vertically from the platform and secondly, we want the rocket to launch without any obstructions. Two such concepts are shown in Figs. A.4.2.1.3.2 and A.4.2.1.3.2.3.

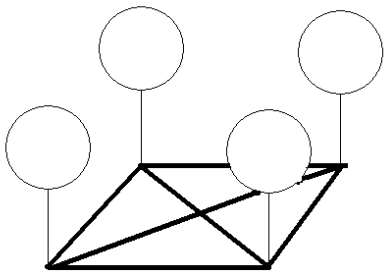

Fig. A.4.2.1.3.2: Concept sketch of balloon apparatus.
(Jerald Balta)

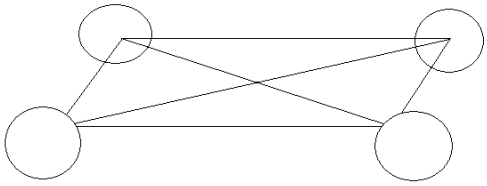

Fig. A.4.2.1.3.3: Concept sketch of balloon apparatus.
(Jerald Balta)

These designs provide a vertical launch platform without having to launch through the balloon. However, the rigid bars in both concepts would take too much stress from winds at high altitudes. A stress analysis can be found in Section A.5.2.6.2. Similar multi-balloon concepts can

also be considered but run into the same stress and complexity issues. Therefore, we are left with a single balloon design where we launch through the balloon. With this design, we assume the launch to be vertical and will be launching through the balloon.

The second aspect in our design to refine is the gondola. Consider here two ideas for carrying the rocket. The first involves hooks being latched onto the rocket to secure it to the balloon. The other involves holding the rocket in some kind of basket. This basket serves as the launch platform for the rocket. After research, we discovered that a launch rail must be included with the gondola in order to control the launch of the rocket. This means that the hook design would not work. Therefore, our gondola design is based on the basket concept.

In order to help determine power and tracking system requirements, it is required for us to know the approximate rise time and downrange drift distance of the balloon. This can be done using simple force balances to determine the forces acting on the balloon and then iterating until the launch altitude of 30,000 meters.

Recalling the force balance in Fig. A.4.2.1.3.1, we must now consider the drag on the balloon as it will now be moving.

We assume that there are no components of wind blowing up or down on the balloon. The lift force can be obtained by multiplying the lift coefficient found using Eq. (A.4.2.1.2.2.5) with the volume found using Eq. (A.4.2.1.2.2.7), resulting in,

$$F_{lift} = C_l \frac{\pi}{6} d^3 g \qquad \text{(A.4.2.1.2.2.9)}$$

where C_l is the lift coefficient in kg/m^3, d is the diameter in m and g is gravitational acceleration, 9.80665m/s^2.

The gravitational force is as defined in Eq. (A.4.2.1.2.2.10) below.

$$F_{gravity} = mg \quad \text{(A.4.2.1.2.2.10)}$$

where m is the total mass of everything the balloon is carrying in kg and g is gravitational acceleration.

The drag force on the balloon is defined in Eq. (A.4.2.1.2.2.11) below.

$$F_{drag} = \tfrac{1}{2}C_D\rho V^2 A \quad \text{(A.4.2.1.2.2.11)}$$

where C_D is the classical drag coefficient of the balloon with no units, ρ is the density of the atmosphere in kg/m^3, V is the vertical velocity of the balloon in m/s and A is the cross sectional area of the balloon in m^2.

The force balance of the balloon is then,

$$ma = F_{lift} - mg - \tfrac{1}{2}C_D\rho V^2 A \quad \text{(A.4.2.1.2.2.12)}$$

We make the initial assumption that the balloon has a drag coefficient of 0.2. Furthermore, in order to simplify calculations, the drag coefficient is assumed to be constant throughout the rise to 30 km. The increasing cross sectional area can be obtained by recalculating the diameter using Eq. (A.4.2.1.2.2.8) at any time period during the rise to 30 km. The drag term must be constrained such that it does not exceed the lift term. When the drag and lift are equal, the balloon has reached terminal velocity and will experience no acceleration.

The density of the atmosphere can be calculated using the barometric atmosphere model. This leaves the velocity as the only unknown in the force balance.

This problem is an ordinary differential equation that can be solved using computational iteration along a small time step. Rearranging the terms in Eq. (A.4.2.1.2.2.12) and substituting for the lifting force, we obtain the following,

$$a = (F_{buoyancy} - \tfrac{1}{2}C_D\rho V^2 A)/m \quad \text{(A.4.2.1.2.2.13)}$$

where the $F_{buoyancy}$ is the difference between F_{lift} and mg.

We now assume the acceleration to be constant during a small time step and use the constant acceleration formula.

$$x = x_0 + v_0 t + \tfrac{1}{2}at^2 \quad \text{(A.4.2.1.2.2.14)}$$

where x_0 and v_0 are the initial displacement and velocity respectively and t is the time over which the formula is used. Using a time step of one second, we then have,

$$\Delta x = x_{previous} + v_{previous} + \tfrac{1}{2}a \quad \text{(A.4.2.1.2.2.15)}$$

and

$$\Delta v = v_{previous} + a \quad \text{(A.4.2.1.2.2.16)}$$

These two equations can be iterated from $x = 0$ until $x = 30000$ in order to determine the time t required to reach the launch altitude.

Now looking at the horizontal motion of the balloon, we can see that there is only one horizontal force acting on it as seen in Fig. A.4.2.1.3.2.4 below.

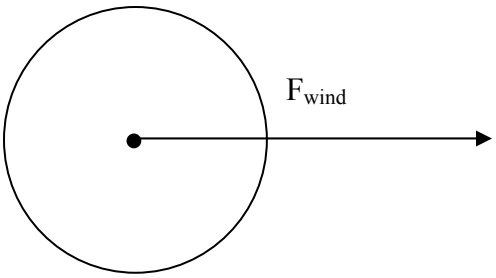

Fig. A.4.2.1.3.2.4: Horizontal free body diagram of the balloon (William Ling)

Due to the fact that the balloon will not maintain a constant spherical area from the side view, we instead assume that the frontal area will be the maximum circular area at an altitude of 30,000 m. This assumption will result in an underestimation of the drift distance due to a higher drag term. However, it should still allow for a magnitude approximation of the drift distance.

Although it may seem that the balloon may continue to accelerate to infinity due to the presence of only a single force, a look at the equations behind the wind force will tell us otherwise.

$$F_{wind} = \tfrac{1}{2} C_D \rho V^2_{relative} A_{max} \quad \text{(A.4.2.1.2.2.17)}$$

where C_D is the classical horizontal drag coefficient with no units, ρ is the density of the atmosphere in kg/m^3, $V_{relative}$ is the relative wind velocity in m/s and A_{max} is the maximum spherical area of the balloon in m^2. As with the analysis of the vertical motion, we assume the horizontal drag coefficient of the balloon to be constant at 0.2.

The term of interest here is the relative velocity. If we consider motion in one dimension with a constant wind blowing on the balloon, as the balloon accelerates, intuition tells us that the relative wind acting on the balloon will decrease. One may think of an analogous example such as blowing at velocity v on a piece of paper travelling away from you at velocity v. The paper will experience no net force from your futile attempts to accelerate it. Due to the force being directly equated to this relative wind, it stands that the balloon should accelerate until it matches the wind velocity at which point there is no force acting on it.

Now that we understand the basic physics behind the horizontal motion, we can do a similar iteration as with the rise time in order to determine the drift range. Eqs. (A.4.2.1.2.2.15) and (A.4.2.1.2.2.16) may also be used for the horizontal motion. The acceleration in the horizontal direction can be represented by,

$$a = (\tfrac{1}{2} C_D \rho V^2_{relative} A_{max})/m \quad \text{(A.4.2.1.2.2.18)}$$

where all variables are as previously defined and the acceleration is in m/s^2.

By determine the motion in the North-South and East-West directions separately using a time step of one second, we then have a three dimensional picture of the motion of the balloon with the z axis pointing upwards and the North-South and East-West directions being x and y respectively.

We will first look at the results in the vertical direction of the balloon. By iterating the equations of motion for the 5 kg payload case with a gross lift off weight of 6,373 kg and a gondola weight of 338.32 kg, we obtain the following results.

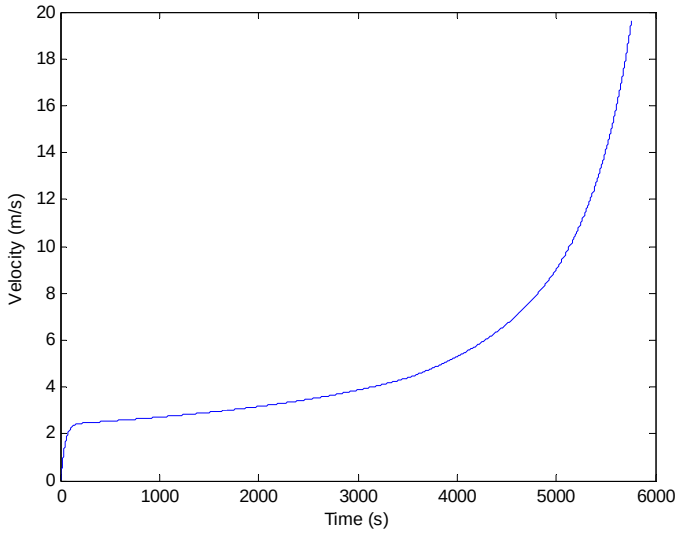

Fig. A.4.2.1.3.5: Change in the balloon's vertical velocity over time.
(William Ling)

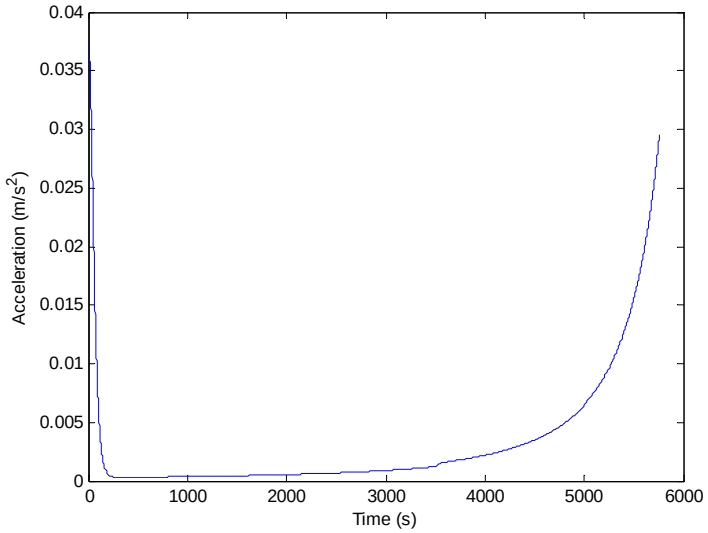

Fig. A.4.2.1.3.6: Change in the balloon's vertical acceleration over time. (William Ling)

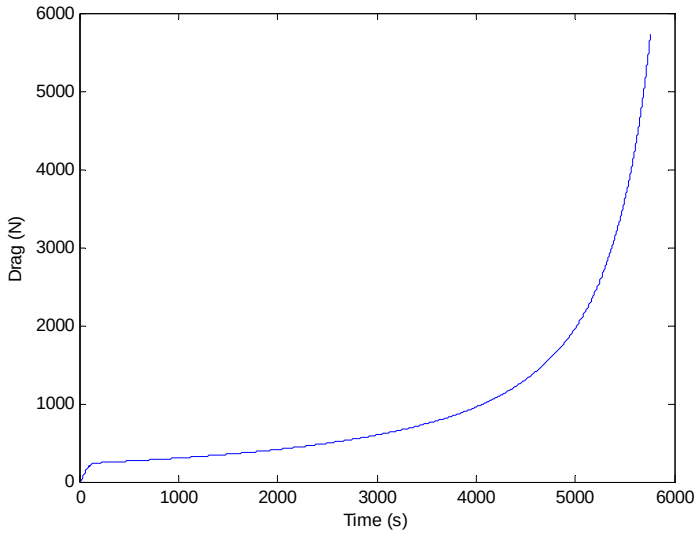

Fig. A.4.2.1.3.7: Change in the balloon's vertical drag over time. (William Ling)

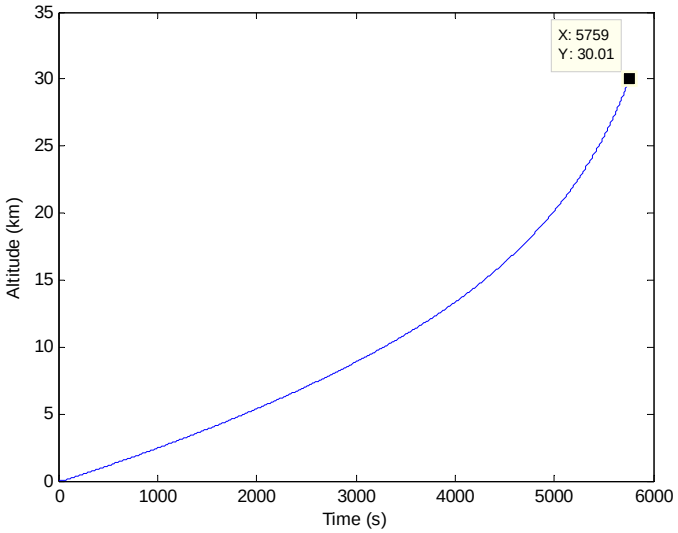

Fig. A.4.2.1.3.8: Change in the balloon's altitude over time.
(William Ling)

From Fig. A.4.2.1.3.5, we can see that the balloon reaches terminal velocity shortly after release. This is reflected in Fig. A.4.2.1.3.6 where the acceleration quickly decreases after takeoff. This suggests that throughout the majority of the rise, the balloon is limited to its terminal velocity and hence by the density of the atmosphere and the drag due to the size of the balloon. Observing Fig. A.4.2.1.3.7, we see that as the balloon begins to gain altitude and the density decreases, the drag of the balloon, which is equal to the lift force of the helium during terminal velocity, rises.

Fig. A.4.2.1.3.8 shows that it takes 5,759 seconds, or 1 hour 36 minutes, for the balloon to reach 30 km in this case. This is slightly lower than, but comparable in magnitude to high altitude balloons such as the NASA Ultra Long Duration Balloon.[4] This lower rise time is likely due to the fact that we assume a constant drag coefficient for the balloon.

We will now look at the motion of the balloon in the horizontal plane. The motions in both the North-South and East-West directions are similar and so we will only analyze the results in the East-West direction. A random wind profile with a random number of gusts of varying strength is generated for each simulation using the wind model presented in Section A.6.2.1.4. The generated wind profile for the East-West direction in this simulation is shown in Fig. A.4.2.1.3.9.

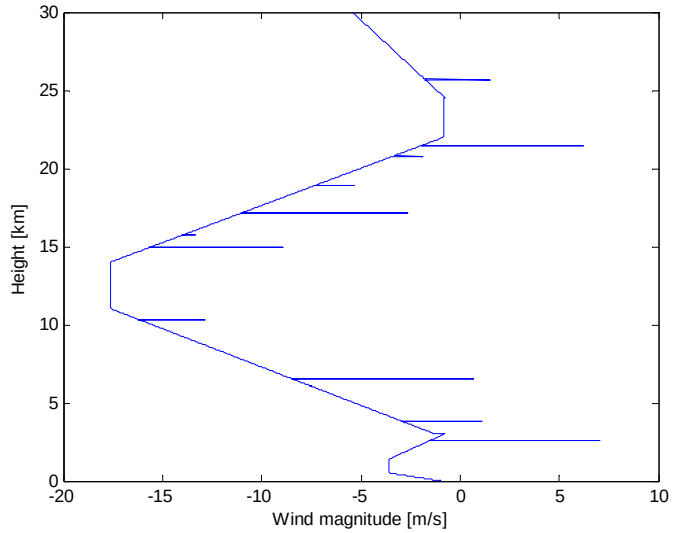

Fig. A.4.2.1.3.9: Random East-West wind profile with random gusts implemented.
(Allen Guzik, Kyle Donahue)

The negative values on Fig. A.4.2.1.3.9 represent wind blowing from west to east. Using this wind profile, we then iterate and solve for the downrange drift distance, velocity and drag. These are shown on the following pages.

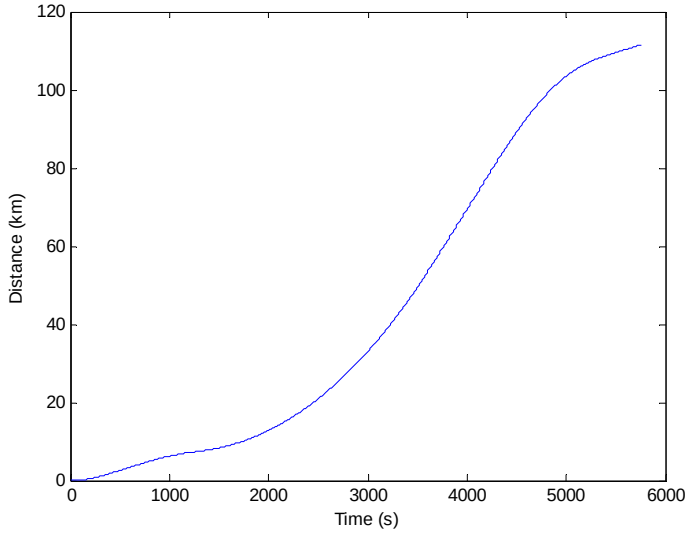

Fig. A.4.2.1.3.10: Change in the balloon's East-West downrange distance over time.
(William Ling)

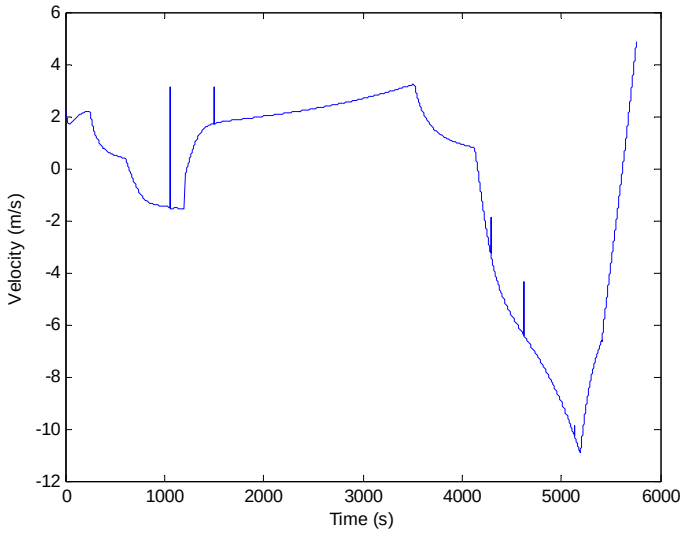

Fig. A.4.2.1.3.11: Change in the balloon's East-West velocity over time. (William Ling)

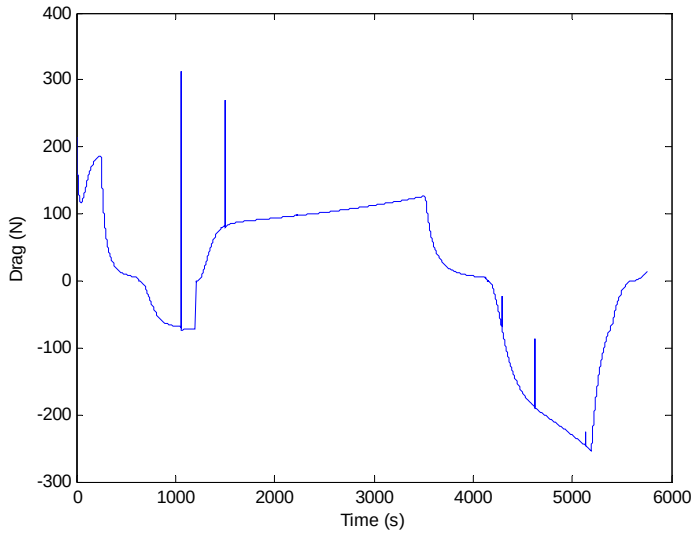

Fig. A.4.2.1.3.12: Change in the balloon's East-West drag over time. (William Ling)

Looking at Fig. A.4.2.1.3.10, we see that the majority of the drift occurs in the center region. This can be explained by comparing it with the wind profile in Fig. A.4.2.1.3.9. For very low and very high altitudes, there is relatively little wind present. The majority of the wind can be seen to occur at approximately 5 to 20 km from the ground. Furthermore, as the density of air decreases the higher you go, the wind blowing will push the balloon less.

Fig. A.4.2.1.3.11 and A.4.2.1.3.12 show the acceleration in the 5 to 20 km altitude range. At around 3,500 to 5,500 seconds, the balloon experiences the highest values of drag throughout the flight. Looking back at Fig. A.4.2.1.3.8 which shows the altitude of the balloon with time, it can be seen that this time corresponds to the altitude range of 5 to 20 km where the majority of the wind is present.

Remember that we assume the drag coefficient of the balloon both in the vertical and horizontal directions to be constant at 0.2. We can verify this assumption by calculating the Reynolds number using the following equation,

$$Re = (Vd)/v \qquad \text{(A.4.2.1.2.2.19)}$$

where V is the velocity of the balloon in m/s, d is the diameter of the balloon in m and v is the kinematic viscosity of the atmosphere in m^2/s. The kinematic viscosity has a temperature relation and can be approximated using the following equation interpolated from experimental data by James Ierardi.[2]

$$v = -1.1555E\text{-}14T^3+9.5728E\text{-}11T^2+3.7604E\text{-}8T-3.4484E\text{-}6 \qquad \text{(A.4.2.1.2.2.20)}$$

where T is the temperature of the atmosphere in Kelvins and can be calculating using the barometric atmosphere. The Reynolds number can then be calculated over the rise time of the balloon for both the vertical and horizontal motions. These are plotted in Figs. A.4.2.1.3.13 and A.4.2.1.3.14.

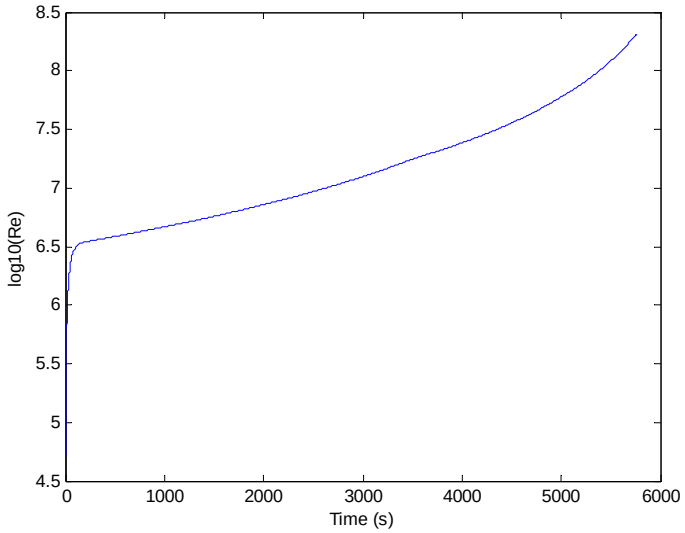

Fig. A.4.2.1.3.13: Change in the balloon's vertical Reynolds number over time. (William Ling)

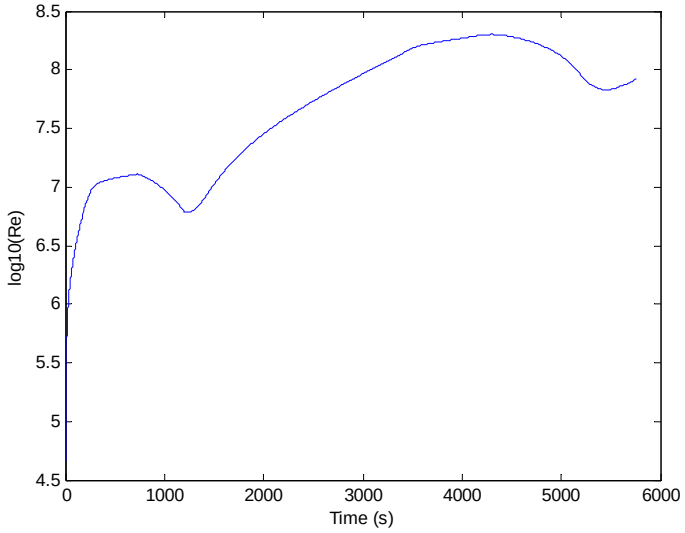

Fig. A.4.2.1.3.14: Change in the balloon's East-West horizontal Reynolds number over time. (William Ling)

It can be seen that the Reynolds number in both cases are in the range of 10^6 to 10^8.25. Since the balloon was approximated as a sphere, we can make use of the readily available drag coefficients for spheres as illustrated in Fig. A.4.2.1.3.15 below.[5]

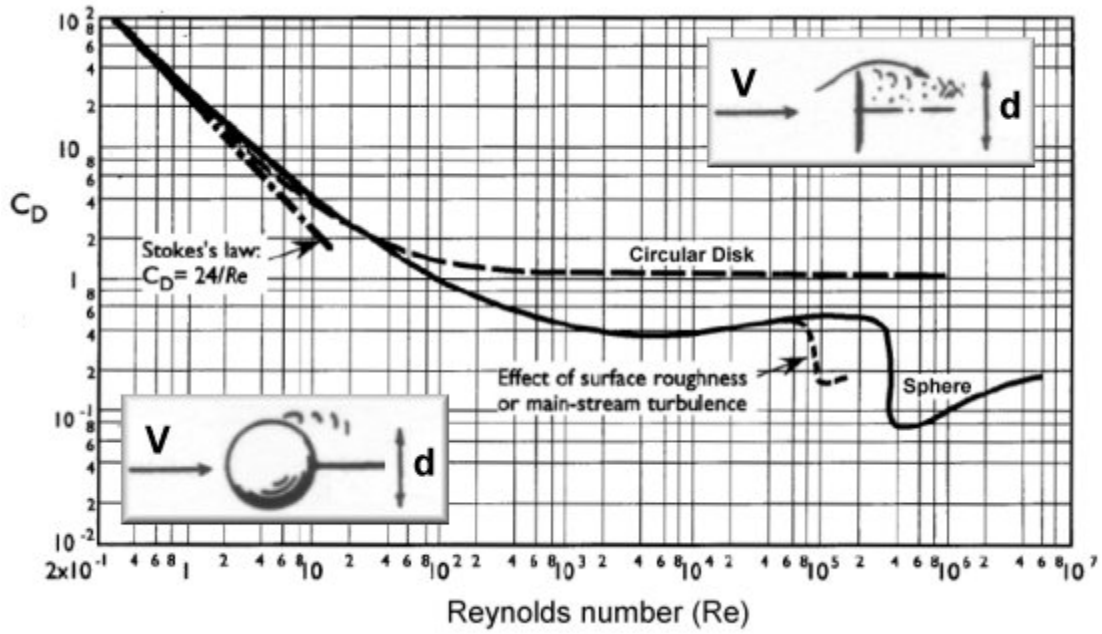

Fig. A.4.2.1.3.15: Drag coefficient of a sphere at varying Reynolds numbers.
(William Ling)

From Fig. A.4.2.1.3.15, the Reynolds number of the balloon is seen to lie almost completely to the left of the plot in the turbulent region where the drag coefficient is approximately 0.2. This demonstrates that the assumption of a constant drag coefficient of 0.2 is valid.

References

[1] Gizinski, Stephen J. and Wanagas, John D., "Feasibility of a Balloon-Based Launch System," *AIAA International Balloon Technology Conference,* Albuquerque, NM, 1991

[2] Tangren, C.D., "Air Calculating Payload for a Tethered Balloon System," *Forest Service Research Note SE-298*, U.S. Department of Agriculture - Southeastern Forest Experiment Station, Asheville, North Carolina, August 1980.

[3] Smith, M.S. and Cathey, H.M. Jr., "Test Flights of the Revised ULDB Design," AIAA Paper 2005-7471, September 2004.

[4] Ierardi, J., "Kinematic Viscosity of Air vs. Temperature," James Ierardi's Fire Protection Engineering Site [online], URL: http://users.wpi.edu/~ierardi/PDF/air_nu_plot.PDF [cited 23 March 2008].

[5] "Drag of Cylinders & "Cones," Aerospaceweb [online], URL: http://www.aerospaceweb.org /question/aerodynamics/drag/drag-disk.jpg [cited 23 March 2008].

A.4.2.1.3 Conventional Gun

One of the methods for quickly launching into Low Earth Orbit is to use a conventional gun which uses some form of a high explosive charge through a gun to launch the system. Our team looked at this type of launch system and performed a feasibility study. This configuration was not chosen in the end due to several limiting factors.

Conventional guns have been used as high altitude research launchers in the past, specifically, in the 1960's during the HARP (High Altitude Research Program.)[1] In this program, a Navy 16 inch conventional gun was used to fire a rocket carrying a payload to a certain altitude, at which point the rocket would fire in order to get a final boost into orbit. The program had several very attractive features that would have worked well for our project. The first would be the high turnaround rate. Some predictions are that the gun could fire at a rate of approximately once an hour, which would greatly reduce ground time and allow a high volume of vehicles to be put into orbit.

A second attractive point of the conventional gun is the relative simplicity of the actual launch vehicle. The initial launch would be using a very large barrel gun with a semi-standard explosive charge. The projectile would then be a rocket with a form of a propulsion system (most likely solid) that would fire and take the small payload into orbit. Since our satellite is so small and has a low mass, this system could be able to fit within the gun in order to be launched.

There was one main reason why this configuration was not finally chosen even with the very attractive qualities. This has to due with the inherent nature of the gun. The projectile would be accelerated at a very high rate in order to get the muzzle velocity needed to get to a high altitude. In the HARP program, estimates were that the launch vehicle would need to withstand approximately 13,000 g's.[1] This g-load was determined to be too high for our system and components. Problems arise with these extreme g's during launch including integrity of materials, sensitivity of electronics, and cracking of solid propellant. In order to get the structure and electronics to withstand these high forces, it was determined that it would be too costly in the long run and would limit the satellites that would be put into orbit using this system. The main theme of the project is to allow groups to cheaply put small satellites into orbit, and by limiting

the capabilities of the satellites that would be launched, we determined that this conventional gun was not an attractive launch type.

References

[1] Wade, Mark, "Martlet 4," [http://www.astronautix.com/lvs/martlet4.htm. Accessed 1/12/08.]

A.4.2.1.4 Rail Guns

Our team looked at the unconventional orbital launch system railguns. A railgun is a device that uses electricity and magnetism to accelerate an object to very high speeds. This application initially looked like an attractive launch system for our project, but was finally dismissed after some reviews.

There are several types of railguns that were looked at, mainly coilguns and railguns. A railgun uses rails that the projectile rides on through the gun. A coilgun is a device that surrounds the projectile in a loop and provides a magnetic field that forces the projectile through the coil. Throughout the analysis, both railguns and coilguns were investigated as possible launch systems.

One of the main draws of using a railgun launch system is the fact that a smaller vehicle can be used due to the high velocity that can be obtained from the electric acceleration system. The system uses strictly electricity to propel its projectile to the high velocity, allowing the system to be located on ground and not having to rely heavily on fuels within the launch vehicle.

What made the launch system attractive with the electricity was also one of its main limiting factors. The energy required to launch the vehicle is extremely high and almost un-realistic in terms of energy supply. Another draw-back of the system is the extremely high aerodynamic heating on the nose and body of the launch vehicle due to the high velocities at low elevation in the lower atmosphere. The amount of energy required was calculated using several different equations that were found using basic electricity equations and derivations from Jengel and Fatro.[1] Equation A.4.2.1.4.1 is used for finding the amount of current needed for launch.

$$I = \frac{v^2 * m}{2 * D * L * B} \qquad \text{(A.4.2.1.4.1)}$$

where I is the current in Amperes, v is the muzzle velocity in m/s, m is the mass of the projectile in kg, D is the muzzle length in meters, L is the distance between the two rails in meters, and B is the electromagnetic field intensity in Teslas. In the analysis, B was assumed to be 10 T, D, L, and v were varied according to desired values, and m was assumed to be 100 kg. The voltage required was calculated using Equation A.4.2.1.4.2.

$$V = v*B*L \qquad (A.4.2.1.4.2)$$

where V is the voltage in Volts and all other variables are described above. With the voltage and current, the power could be calculated using Equation A.4.2.1.4.3

$$P = V*I \qquad (A.4.2.1.4.3)$$

where P is the power in Watts. The force put onto the projectile as it accelerates through the muzzle was calculated using Equation A.4.2.1.4.4

$$F = P*B \qquad (A.4.2.1.4.4)$$

where F is the force on the projectile in Newtons. Finally, the acceleration of the projectile was calculated using Equation A.4.2.1.4.5

$$a = F/(m*9.80665) \qquad (A.4.2.1.5.5)$$

where a is the acceleration of the projectile in g's.

Railguns also have high accelerations like a conventional gun. One way to try to lower the acceleration is to lengthen the actual railgun. In order to bring down the acceleration force to approximately 100 g's, the rail gun would have to be approximately 2.2 km long. This length is unrealistic given the complexities of the rail gun system and the extremely tight tolerances needed to hold the high velocity projectile riding the rails.

All of these different factors can be seen in Table A.4.2.1.4.1 which summarizes the different components of the railgun. These values are a selection of values which gives general values that represents one case. Many different cases were run with various values changing as described above.

Table 4.2.1.4.1 Rail Gun Quantities for LEO Launch

Variable	Value	Units
Muzzle Velocity	5,000	m/s
D	2,000	M
I (Current)	62,500	A
B	10	Tesla
Acceleration	637	g's
Voltage	50,000	V
Power	3,125,000	kW-hr

When the length of the rails D is shortened to a reasonable length of rail, the acceleration goes much higher as can be seen in Table 4.2.1.4.2.

Table 4.2.1.4.2 Rail Gun Quantities for LEO Launch

Variable	Value	Units
Muzzle Velocity	5,000	m/s
D	100	M
I (Current)	1,250,000	A
B	10	Tesla
Acceleration	12,724	g's
Voltage	50,000	V
Power	3,450,000	kW-hr

As can be seen, the figures in both the tables are extremely high. The g load is too high for a feasible launch vehicle design, and the electricity demands are unrealistic and impractical. In order to get such high values for the electricity, a very sophisticated and large capacitor system as well as a power producing system would need to be invested, making it difficult to keep costs down.

Due to all of the negative factors mentioned, it was determined that rail guns, while initially an attractive alternative for a launch system, were too expensive through the development and unrealistic to make, and were therefore not selected.

References

1. “Jengel and Fatro’s Rail Gun Page,” April 24, 2002, [http://home.insightbb.com/~jmengel4/rail/rail-intro.html Accessed 22 January 2008]

A.4.2.2 Propellants

A.4.2.2.1 Liquid Research

Liquid propellant is rocket fuel, but in a liquid state which consists of oxidizer and fuel. For the final design we do not use liquid propellant in any of the stages of the launch vehicle because of the risks and costs associated with liquid propellant. However, we had considered liquid propellant at first because of the high performance it provides. We researched various cryogenic and storable liquid propellants, starting with Table A.4.2.2.1 which shows all of the liquid propellant choices we had analyzed for selection.[1]

Table A.4.2.2.1 Liquid Oxidizer and Fuel Possibilities

Oxidizer	Fuel	Specific Impulse (Sea Level)
Liquid Oxygen	Liquid Hydrogen	381
	Liquid Methane	299
	Ethanol + 25% water	269
	Kerosene	289
	Hydrazine	303
	MMH	300
	UDMH	297
	50-50	300
Liquid Fluorine	Liquid Hydrogen	400
	Hydrazine	338
FLOX-70	Kerosene	320
Nitrogen Tetroxide	Kerosene	267
	Hydrazine	286
	MMH	280
	UDMH	277
	50-50	280
Red-Fuming Nitric Acid (14% N_2O_4)	Kerosene	256
	Hydrazine	276
	MMH	269
	50-50	270
Hydrogen Peroxide (85% concentration)	Kerosene	258
	Hydrazine	269
Nitrous Oxide	HTPB (solid)	248
Chlorine Pentafluoride	Hydrazine	297

Cryogenic fuels must be kept at extremely low temperatures to maintain liquid form. Some examples are liquid oxygen and liquid hydrogen. Liquid oxygen must be kept at temperatures lower than -183^{o}C and liquid hydrogen must be kept at temperatures lower than -253^{o}C.[2] Because of the low temperatures of the fuel, storage and transport of cryogenic fuels requires additional constraints on the vehicle in comparison with storable fuels. The lower temperature requires insulation or special material for tanks, propellant feed lines, and engine components. Ambient temperature outside the tank is always much higher than that of the cryogenic propellant inside the tank. Thermal gradients cause additional stress on the tank structure and heat transfer between the two. Heat transfer from ambient conditions to fuel causes boil-off which can lead to the over pressurization of the tanks.[2] Therefore, we need a pressure release valve on the tanks to prevent leakage or explosion.

Not only does boil-off cause over pressurization, but may cause a loss of fuel. Cryogenic fuels cannot be used for launches that require a long waiting time and cannot be ready instantaneously. Due to the length of time for our balloon launch, boil-off could be so extensive that the rocket would need to carry excessive propellant to accomplish our goals. It is a lengthy process to fill a rocket with cryogenic fuel. The main process as listed.[2]

- Expulsion of water or solid particles from pressurant lines, injectors, and tanks.
- Attaching and detaching hoses
- Checking seals for leaks
- Inspecting hoses
- Prechill of cryogenic components and propellant pipes.
- Venting gasses formed by prechill to avoid over pressurization.

Also, the whole process must be completed by a team of specially trained personnel wearing hazardous material suits that protect them from spilled fuel. Specially trained personnel are required as standby during the process should a major spill or leak occur.

During flight the boiling temperature of cryogenic propellants is raised slightly due to the pressurization of the fuel delivery system. Additional pressure allows the cryogenic fuel to

remain in liquid form even though it is being exposed to a greater amount of heat from the burning of the propellants. However, when transferring fuel to the rocket, the temperature must remain below the boiling temperature at atmospheric pressure because pressurizing the transfer hoses would be costly and dangerous.

While cryogenic fuels are harder to store and maintain, the benefits of using them is found in the performance characteristics. While general bipropellant fuels usually have a specific impulse (Isp) range of 300-460 seconds. Cryogenic fuels are known for having high Isp in relation to other bipropellant fuels.[3] Fuels that may be used with either a cryogenic or storable oxidizer usually have a higher performance when used with a cryogenic oxidizer.[4] Also, some cryogenic propellants offer an added benefit of less pollution.

Due to the expense of handling and preparing for the use of cryogenic fuels, the main costs are not a result of the cost of propellant, but the cost of additional systems and handling. Specialized equipment, launch pad personnel, and additional time needed for cryogenic fuel loading make the cost of the fuel seem negligible in comparison. Therefore, cryogenic systems require a cost modifier added to account for the additional expenses of working with these propellants.
Cryogenics, while a far superior fuel in performance, create cost problems that are well beyond the spectrum of our project. Cryogenic fuels are furthered analyzed in the Model Analysis simulations, but were regarded as an improbable propellant selection.

The other type of liquid propellant we considered in our propellant selection analysis is storable liquid propellants. We can safely and easily store these types of propellants in a reasonable range of pressures and temperatures without risk of corrosion and/or evaporation. Unlike cryogenic propellants, we can place storable liquid propellants in a sealed container at room temperature for long periods of time. Some are hypergolic which simplifies the engine operation even more. High toxicity is just one of the disadvantages of liquid propellants. Handling and transportation of some propellants cause environmental concerns. Additionally, storable propellants typically have lower Isps than cryogenic propellants.

There exist oxidizers we certainty did not want to use in our launch vehicle such as using liquid fluorine which is highly corrosive, flammable and poisonous. Hence, we did not use any compound that has fluorine. Nitric Acid, HNO_3, is also highly corrosive. Nitrogen tetroxide, N_2O_4, is corrosive, but is the most common oxidizer used in the United States today.[2] Hydrogen Peroxide, H_2O_2, is hypergolic with hydrazine and burns readily with kerosene, RP-1. It decomposes at a slow rate and H_2O_2 produces nontoxic exhaust. There exists many dangerous fuels such as MMH which is toxic when inhaled and when exposed to air, it easily ignites; too volatile for us. UDMH has less toxicity than MMH, but when burned with an oxidizer, it introduces a lower Isp than pure hydrazine.[2] However, because of their carcinogenicity, we dropped UDMH and MMH from our analysis. Hydrazine is an excellent storable fluid, but it fails as a good fuel choice because of its toxicity and carcinogenicity. It is hypergolic which is why we thought a H_2O_2/Hydrazine combination was most appropriate. Nontoxic kerosene is easy to handle and low in cost.

Using the above information, we narrowed our storable propellant choices to the following: H_2O_2/Hydrazine, H_2O_2/RP-1, and N_2O_4/RP-1. The performance of our propellants is the driving force of our mission and what we used to select a storable propellant. Hydrazine combined with RP-1 has an Isp of 282,[5] but due to the carcinogenicity of hydrazine we decided not to select that particular propellant. We know that RP-1 is a good fuel to use, could easily work with almost any oxidizer, and offers a good performance. N_2O_4/RP-1 has a slightly higher Isp, 267, than H_2O_2/RP-1, which has an Isp of 258,[1] our mission is to design a vehicle a university may launch and keep safety in mind.

We select H_2O_2/RP-1 as our storable propellant choice because it provides a decent Isp value, a cheap cost and a reassurance that it is relatively safe to use. All the other choices are either too expensive or too dangerous to use.

References

[1] Braeunig, R., A., "Rocket Propellant Performance," *Basic Space Flight: Rocket Propellants ,* 2008. [http://www.braeunig.us/space/propel.htm. Accessed 2/1/08.]

[2] Sutton, G., Biblarz, O., Rocket Propulsion Elements, John Wiley & Sons, Inc., New York, NY, 2001.

[3] Hrbud, Ivana., Rocket Propulsion – AAE 439 Class Notes., West Lafayette, IN, 2007.

[4] Humble, R. W., Henry, G. N., Larson, W. J., Space Propulsion Analysis and Design, McGraw-Hill, New York, NY, 1995.

[5] Wade, Mark, "H2O2/Hydrazine," 1997-2007. [http://astronautix.com/props/h2oazine.htm. Accessed 1/22/08.]

A.4.2.2.2 Hybrid Research

We also consider hybrid rocket motors which are a joining of a liquid and solid propulsion system. Using a liquid oxidizer and a solid fuel section a hybrid motor combines both systems into a viable engine. There are a small fraction of hybrid motors which use a liquid fuel and a solid oxidizer. Hybrid motors will generally perform in the region between bipropellant systems and solid rocket motors. Tables 4.2.2.2.1 and 4.2.2.2.2 below show several possible combinations of liquid oxidizers and solid fuels.

Table 4.2.2.2.1 Specific Impulses for Liquid Oxygen and Solid Fuel Combinations[1]

Pressure (psi)	O/F	HTPB	PBAN	PU	PMMA	PEG	PGA	GAP	AMMO	BAMO
150	0.8	177.2	185.0	170.3	190.9	197.3	190.4	224.2		221.5
	1.4	215.1	222.7	218.4	216.9	218.1	204.5	212.0		216.3
	2.0	231.3	226.3	217.8	209.2	209.5	196.2	200.9		205.4
300	0.8	197.5	204.6	190.0	210.6	217.9	210.7	252.0		246.5
	1.4	237.0	246.8	243.1	244.2	245.8	231.0	239.4		244.3
	2.0	259.2	255.3	246.0	236.5	236.7	221.3	226.5		231.8
500	0.8	210.7	217.1	203.1	222.5	230.4	223.1	269.3		261.5
	1.4	250.1	261.2	258.0	261.3	263.3	248.1	257.1		262.5
	2.0	276.2	273.7	264.3	254.2	254.3	237.5	242.8		248.8

Footnotes: All specific impulses are in units of seconds. O/F is the oxidizer-to-fuel ratio

Table 4.2.2.2.2 Specific Impulses for Hydrogen Peroxide and Solid Fuel Combinations[1]

Pressure (psi)	O/F	HTPB	PBAN	PU	PMMA	PEG	PGA	GAP	AMMO	BAMO
150	0.8	151.3	152.8	146.5	149.9	153.6	144.5	197.6		180.3
	1.4	161.8	164.0	163.2	177.2	182.3	177.4	212.2		203.9
	2.0	177.2	187.4	187.2	196.3	199.4	195.0	215.3		212.5
300	0.8	170.8	172.5	165.5	169.4	173.4	163.1	218.0		199.0
	1.4	182.8	184.8	182.7	195.9	201.6	196.3	235.6		225.7
	2.0	196.8	206.8	207.0	217.4	221.0	216.2	240.9		236.3
500	0.8	183.4	185.2	177.7	182.1	186.3	175.2	230.4		210.7
	1.4	196.4	203.0	195.5	207.6	213.4	207.9	249.7		238.8
	2.0	209.6	218.8	219.1	230.3	234.1	229.3	256.6		250.8

Footnotes: All specific impulses are in units of seconds. O/F is the oxidizer-to-fuel ratio

The full name of the solid fuel components are listed below:

HTPB = Hydroxyl Terminated Polybutadiene
PBAN = Polybutadiene Acrylic Acid Acrylonitrile
PU = Polyurethane
PMMA = Polymethyl Mathacrylate
GAP = Glycidyl Azide Polymer
AMMO = Azidomethyl Methyl Oxetane
BAMO = bis Azidomethyl Oxetane
PEG = Polyethylene Glycol
PGA = Polydiethylene Glycol Adipate

Different values are used in the Model Analysis performed by the team. These new values for chamber pressure and specific impulse are found using a thermochemistry analysis (see A.4.2.2.5).

Other types of oxidizers were considered by the propellant selection group, but many were rejected. Due either to their extremely toxic nature (such as Nitric Acid or Nitrogen Tetroxide) or high pressurization requirements (Nitrogen Tetroxide or Gaseous Oxygen).

An advantage of a hybrid motor over a bipropellant system is a reduction in complexity. Hybrid motors will generally have half of the piping, ducts, injectors, and pressurization systems of bipropellant engines. This reduction in complexity helps to reduce the overall cost of a hybrid system when compared to a bipropellant system. However, liquid system requirements will still generally make them more costly than a solid rocket motor.

Hybrid motors are more complex than solid rocket motors and have higher inert masses. However, hybrid motors will have higher specific impulses than solid rocket motors generally making up for their added inert mass. Another advantage of a hybrid motor over the less complex solid motor is the ability to throttle the engine. Solid rocket motors, once ignited, will burn in a pre-designated pattern. Since hybrid motors can control the amount of oxidizer injected into the solid fuel grain, hybrids can control and vary their thrust at anytime during flight. Also as hybrid motors have their oxidizer and fuel separated there is no great risk for spontaneous combustion of the propellant, a major hazard for solid rocket motors.

When we considered the two main choices for the liquid oxidizer, liquid oxygen or hydrogen peroxide, we weighed the outcome of choosing either system over the other. If we were to select liquid oxygen we would be choosing a cryogenic system which carries with it added complexity due to the extremely low temperatures. If we choose hydrogen peroxide we will have an oxidizer that can be stored at room temperature but lacks the high performance of cryogenic liquid oxygen. As cost is the main driver in our design we chose hydrogen peroxide as the oxidizer for our hybrid systems. The reduced complexity of a hydrogen peroxide system will also help to reduce the overall cost of our launch vehicle.[2]

Selecting the proper solid fuel component to accompany our choice of a hydrogen peroxide oxidizer proved more difficult. For our selection of a solid propellant for the hybrid system we wished to select a fuel that had been tested extensively by other designers. In the end this criteria meant the selection of Hydroxyl Terminated Polybutadiene, more commonly referred to as HTPB. Even though it is amongst the lowest specific impulse solid fuels available HTPB is relatively easy to cast and is less expensive than other propellants.

Using all of the aforementioned criteria for design of our hybrid system our final designs use a hydrogen peroxide oxidizer and HTPB fuel. The final value for the specific impulse of our selected propellants is 337.6 seconds at a chamber pressure of 300 psi.

References

[1] Helmy, A.M., "Investigation of Hybrid Rocket Fuel Ingredients," AIAA Paper 94-3174, June 1994.

[2]Sutton, George P., Biblarz, Oscar. "Hybrid Propellant Rockets: Applications and Propellants," *Rocket Propulsion Elements*, 7th ed. Wiley-Interscience, New York, 2001, pp. 580-585

Author: Stephen Bluestone

A.4.2.2.3 Solid Research

Solid Rocket Motors (SRMs) are among the oldest and simplest of launch vehicle engines. In an SRM the oxidizer and fuel are combined into a single grain which is then cast into the motor casing. With the addition of a nozzle and an igniter the SRM is essentially ready to fire. Being a simple design SRMs are usually one of the simplest motors to design and build. Simplicity also leads to SRM being among the cheapest of propulsion systems. However, a solid rocket motors main drawback is low specific impulse. Table 4.2.2.3.1 below shows several solid fuel combinations and associated performance criteria.

Table 4.2.2.3.1 Solid Fuel Performance[1]

Fuels (Solids)	Density (kg/m^3)	Flame Temp (K)	Isp (seconds)
DB	1605.43	2550	220-230
DB/AP/AL	1799.19	3880	260-265
DB/AP-HMX/Al	1799.19	4000	265-270
PVC/AP/Al	1771.51	3380	260-265
PU/AP/Al	1771.51	3440	260-265
PBAN/AP/Al	1771.51	3500	260-263
CTPB/AP/Al	1771.51	3440	260-265
HTPB/AP/Al	1854.55	3440	260-265
PBAA/AP/Al	1771.51	3440	260-265
AN/Polymer	1467.03	1550	180-190

The full name of the solid fuel components are listed below:

Al = Aluminum
AN = Ammonium Nitrate
AP = Ammonium Perchlorate
CTPB = Carboxyl-terminated Polybutadiene
DB = Double-base
HMX = Cyclotetramethylene Tetranitramine
HTPB = Hydroxyl-terminated Polybutadiene
PBAA = Polybutadiene-acrylic acid polymer
PBAN = Polybutadiene-acrylic acid-acrylonitrile terpolymer
PU = Polyurethane
PVC = Polyvinyl Chloride

As can be seen in table 4.2.2.3.1 the specific impulse values for the various solid fuels are nearly identical with a few exceptions. In general these solid fuels have a specific impulse around 260 to 265 seconds. All of the fuels also have a high density allowing for the storage of a large amount of propellant in a relatively small volume.

Solid rocket motors will always have an oxidizer (generally Ammonium Perchlorate) and a fuel cast into the grain. But in many designs other materials may be added to the grain to increase performance or enhance certain aspects of the rocket. Energetic plasticizers such as HMX may be added to increase performance of the fuel grain.[1] However, since many of the fuels shown above have relatively the same performance it is more of a design choice to select one fuel over another. More in depth design would allow us to perfect a combination of oxidizers, fuels, and materials but this would require extensive computational optimization.

Another significant aspect of solid rocket motor (and hybrid motor) design is the port design in the fuel grain. Thrust generated by the motor is directly dependant on the surface area of the fuel grain exposed to burning. The shape, arrangement, and area of ports will have a significant affect on the thrust history of the SRM. Depending on the mission profile and thrust requirements the ports in the grain can be designed to give more or less thrust as required. Design of ports, both axial and radial, is extremely complex and is beyond the scope of our project. With more time we believe that it would be possible to explore simple port designs.

As with the hybrid propellant selection, solid propellant selection came down to knowledge of the materials. Since the majority of solid propellants found have nearly the same specific impulse we made a decision to use HTPB/AP/Al as our solid propellant.

References

[1] Sutton, George P., Biblarz, Oscar, "Solid Propellant Rocket Fundamentals," *Rocket Propulsion Elements*, 7th ed., Wiley-Interscience, New York, 2001, pp. 417-467

A.4.2.2.4 Selection

Our next step in analysis is to select the final propellants from each category described in Sections A.4.2.2.1, A.4.2.2.2, & A.4.2.2.3. Limiting the number of propellants for model analysis, we narrowed down the propellants based on specific impulse (Isp) and ease of handling. We ended up with a set of four propellants one in each category; cryogenic, storable, hybrid, and solid. We use this list of propellants in the main Model Analysis simulations which determine final designs of our three launch systems.

The main criteria we considered when selecting the four types of propellants were; Isp, cost of propellant, and handling/safety. We also considered additional complexities in design and cost that could arise with the selection of specific types of fuels.

Specific Impulse (Isp) is one the main items to consider when designing any launch vehicle system. Engine performance is generally specified in terms of Isp and chamber pressure (which can be altered easily in comparison with fuel selection). We naturally want to select a propellant with the highest possible Isp but other considerations, which will be described later, must be taken into account. Table A.4.2.2.4.1 is a list of several propellants and their associated specific impulses.

Table A.4.2.2.4.1 Propellant Specific Impulses

Propellant	Specific Impulse (Isp)	Units
Liquid Oxygen / Liquid Hydrogen (cryo)	380 [1]	Seconds
Liquid Oxygen / RP – 1 (cryo)	291 [1]	Seconds
Liquid Oxygen / Hydrazine (cryo)	300 [1]	Seconds
Hydrogen Peroxide / Hydrazine (storable)	282 [1]	Seconds
Hydrogen Peroxide / RP – 1 (storable)	267 [1]	Seconds
Nitrogen Tetroxide / RP – 1 (storable)	267 [1]	Seconds
Hydrogen Peroxide / HTPB (hybrid, storable)	268 [2]	Seconds
Nitrogen Tetroxide / HTPB (hybrid, storable)	270 [2]	Seconds
Hydrogen Peroxide / GAP (hybrid, storable)	256 [2]	Seconds
DB/AP-HMX/Al (solid)	265 [3]	Seconds
HTPB/AP/Al (solid)	260 [3]	Seconds
DB/AP/Al (solid)	260 [3]	Seconds

Footnotes: All specific impulses are at sea level conditions, these are not Isps used, these were used to aid in propellant selection (see thermo chemistry A.4.2.2.5 for more information)

We can see from table A.4.2.2.4.1 that for our four types of propellants (cryo, storable, hybrid, and solid) specific impulse does not vary greater than ten seconds, with the exception of liquid oxygen / liquid hydrogen. Due to great variation between liquid hydrogen / liquid oxygen and the other cryogenic fuels, we specifically chose liquid oxygen / liquid hydrogen as our cryogenic fuel for Model Analysis simulations. Selection for the other three systems required more analysis.

Generally speaking, the cost of the propellant will be negligible in comparison to the cost of the engine and sub systems of the launch vehicle. In modern rocket design, most propellants are manufactured in bulk quantities which tend to limit costs. However, certain propellants, regardless of propellant price, can be extremely expensive due to the handling costs associated with their use.

The main qualities we consider in the selection of the four propellants are the costs of equipment, personnel, and design alterations associated with the propellant characteristics. Some of the main considerations are:

- Highly Pressurized Propellants
- Low Temperature Propellants (cryogenics)
- Toxicity
- Volatile Nature

Highly pressurized propellants require stronger, and thus, thicker tanks. These thicker tanks are heavier and more costly which makes them detrimental to our design. Propellants under high pressure also pose a safety hazard as they are less stable.

Low temperature propellants pose a problem due to the tank, piping, and engine requiring insulation against the frigid temperatures. This also demands additional weight and cost associated with the insulation. Additional person hours are needed to fill the launch vehicle due to precooling the lines. A potential risk associated with cryogenic systems is boil-off leading to over pressurization of the fuel tanks and pressurant lines. This requires the addition of a bleed system to prevent explosion which increase complexity and cost.

Toxic fuels pose serious risk to personnel and surrounding areas. They require specialized crews and equipment to transport, handle, and load. Fuel leaks can lead to serious health risks to ground personnel and detonation of the launch vehicle in flight could lead to spills over large areas. Some toxic fuels are carcinogenic and may not pose an immediate threat to community but could have lasting effects on health and wellbeing.

Several propellants, mainly solid rocket motors, are in laymen's terms a large bomb. Solid rocket motors are cast with the fuel and oxidizer integrated and only requires a source of ignition. Once ignited the solid rocket motor cannot be stopped from burning. Another potential threat is damage to the propellant grain leading to cracks. These cracks may cause overheating and over pressurization which will ultimately lead to case damage or catastrophic explosion.

Using the aforementioned criteria we chose not to select several fuels as they posed a great risk to the success of our final design or risk to personnel. Fuels with Hydrazine (in all forms) or Nitric Acid were not selected due to their toxic nature. Nitrogen Tetroxide was not selected due to its toxic nature and required pressurization. Other fuels were excluded from selection due to a lack of information for analysis.

Considering the list of propellants and removing those with weak characteristics we arrived upon a selection of our final four propellants. The list is as follows:

1. Cryogenic Bipropellant – Liquid Oxygen and Liquid Hydrogen
2. Storable Bipropellant – Hydrogen Peroxide and RP-1
3. Hybrid – Hydrogen Peroxide and HTPB
4. Solid Rocket Motor – HTPB/AP/Al

These propellants were used in our Model Analysis simulations run by our team. Propellants were varied along with other launch vehicle characteristics to attain our final design.

References

[1] Humble, R. W., Henry, G. N., Larson, W. J., Space Propulsion Analysis and Design, McGraw-Hill, New York, NY, 1995.

[2] Helmy, A. M., "Investigation of Hybrid Rocket Fuel Ingredients," AIAA Paper 94-3174, June 1994.

[3] Sutton, G., Biblarz, O., Rocket Propulsion Elements, John Wiley & Sons, Inc., New York, NY, 2001.

A.4.2.2.5 Thermochemistry Analysis

A.4.2.2.5.1 Chemical Equilibrium with Applications Code

The NASA Chemical Equilibrium with Applications (CEA) code is widely used by students and in industry to calculate the thermochemical properties of a combustion process.[1] In our case, we used the CEA code to calculate engine performance parameters for our launch vehicle.

In our case, CEA was run to calculate specific impulse, c^*, exit pressure, exit Mach number, exit speed of sound, and coefficient of thrust. All performance information can is used to calculate thrust, mass of propellant, and mass flow rate. CEA requires some inputs by the user as listed; chamber pressure, area ratio, propellant, oxidizer to fuel ratio, and temperature of propellants entering combustion chamber. In order for us to work the code, we use historical data to find a reasonable chamber pressure, area ratio, and temperature of propellants entering the combustion chamber.

Chamber pressure is the first calculated because area ratio calculations are dependent on knowing the chamber pressure. We know we are using a pressure fed system requiring a chamber pressure between one and three megapascals for liquid propellant systems.[2] Due to our need to minimize inert mass, we decided to choose chamber pressures not exceeding 2.5 megapascals. Solid propellant systems are known to have chamber pressures of around five to eight megapascals.[2] For the purposes of minimizing mass, we chose six megapascals. Designers generally choose chamber pressures as we did, by using historical data and guessing what would work best for their design. While not a very efficient method, there is no way to predict the ideal chamber pressure until more is known about the engine performance and weight. Calculation requires an iterative process between propulsion, structures, and trajectory.

Now that chamber pressure is known, area ratio may be found. In vacuum conditions, the ideal engine would have an infinitely expanding nozzle.[2] However, that is not possible and so we must balance the mass of the nozzle with the performance. The nozzle must be expanded enough to minimize detriment caused by the nozzle weight. For vacuum conditions, area ratio was chosen as 60.

During ground launch, area ratio must be found so that separation is prevented. Separation causes a loss in engine performance by significantly reducing the area ratio and pressure thrust. By using the Kalt-Bendall equation, we can find the separation pressure.

$$P_{sep} = 0.667 P_{amb} \left(\frac{P_c}{P_{amb}} \right)^{-0.2} \qquad \text{(A.4.2.2.5.1)}$$

where P_c is the chamber pressure, P_{amb} is the ambient pressure, and P_{sep} is the separation pressure.

In order to find an area ratio that is applicable, exit pressure of the nozzle selected must be greater than the separation pressure calculated. In our case, ambient pressure will be atmospheric pressure at sea level. In our case, we find the following first stage area and pressure ratios:

Table A.4.2.2.5 First Stage Area and Pressure Ratios

Propellant	A_{exit}/A_{throat}	P_c/P_{exit}
LOX / LH2	6.497	54.54
H2O2 / RP-1	8.244	63.64
H2O2 / HTPB	8.150	54.12
AP / HTPB / Al	20.00	200.6

The above area ratios were used only in first stage ground launch. For aircraft and balloon it was assumed that the launch vehicle was already high enough to prevent separation.

Lastly, the CEA code needs the temperature in which the propellants enter the combustion chamber. For all but cryogenic fuels, the temperature was assumed ambient temperature (298.15 K). Cryogenic fuels are kept much cooler and therefore, the boiling temperatures of the cryogenic fuels were used. In our case, liquid oxygen enters the chamber at 20.27 K and liquid hydrogen at 90.20 K.[3] These boiling points are imbedded in the CEA code and did not need a separate source.

All other information that would have been needed had we written a code ourselves, heats of formation, gibbs free energy, etc. are found in the CEA code. The built in parameters and

functions make the code very convenient and relevant to our engine computations. Also, the code has the option of calculating performance parameters based on frozen or equilibrium flow. During frozen flow, the constituent products are assumed to remain in that form throughout the nozzle.[3] During equilibrium flow, the constituent products are assumed reform during all possible recombination reactions.[3] Neither of these methods allows for an accurate measure of engine performance parameters, but a mean value is usually used. Therefore, we used the CEA code twice and calculated all engine performance parameters with both methods.

The CEA code proves useful as a tool for us and industry. If CEA were not available to us our engine performance parameters would have been based off frozen flow. The frozen flow assumption would make our launch vehicle heavier and more costly due to lower performance of the fuels we are using.

References

[1] Chao, M., "NASA Chemical Equilibrium with Applications," Marshall Space Flight Center, Alabama, February, 2008. [www.grc.nasa.gov/WWW/CEAWeb. Accessed 1-25-08.]

[2] Humble, R. W., Henry, G. N., Larson, W. J., Space Propulsion Analysis and Design, McGraw-Hill, New York, NY, 1995.

[3] Heister, Stephen D., AAE 539 class., Purdue University, West Lafayette, IN, 1/14/08.

A.4.2.2.5.2 Mixture Ratio Optimization

An important factor in obtaining the best performance from a launch vehicle is optimizing the mixture ratio. In our analysis, we define the mixture ratio as the ratio between mass of oxidizer and fuel. Mixture ratio is also referred to as the oxidizer to fuel ratio. Maximizing the oxidizer to fuel ratio allows the maximum amount of energy release in a reaction. We ran the NASA Chemical Equilibrium with Applications (CEA) code and were able to optimize the oxidizer to fuel ratio for each propellant.

For solid propellants optimization of the oxidizer to fuel ratio is unnecessary. The CEA code was run for different oxidizer to fuel ratios with all other conditions remaining the same. The specific impulses (Isp) and characteristic velocities (c^*) were recorded and charted. After this the maximum was found and we chose that value as our oxidizer to fuel ratio for the rest of the project.

Figure A.4.2.2.5.2.1 shows where the maximum oxidizer to fuel ratios occur for each of the three propellants.

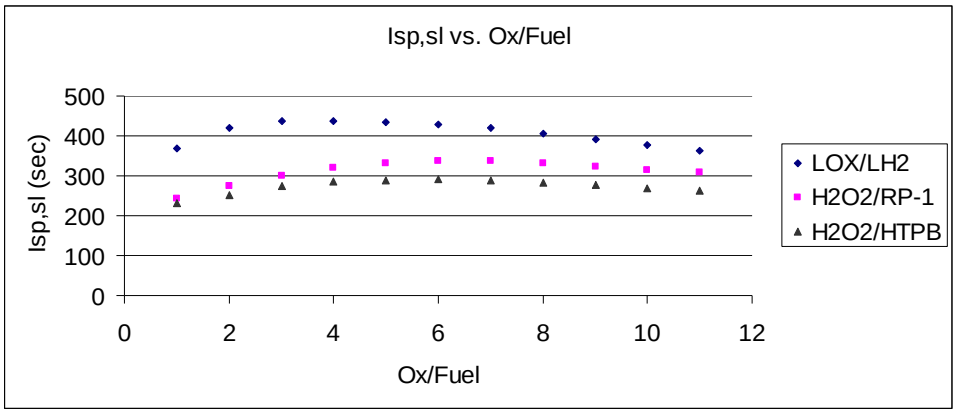

Fig. Section A.4.2.2.5.2.1: Sea level Isp versus oxidizer to fuel ratio.
(Wilcox, Nicole)

In Fig. A.4.2.2.5.2.1, it is clear that the optimum oxidizer to fuel ratios is 3 for liquid oxygen and liquid hydrogen, 6 for hydrogen peroxide and RP-1, and 6 for liquid hydrogen and HTPB. These numbers are illustrated again in Fig. A.4.2.2.5.2.2 for vacuum specific impulses.

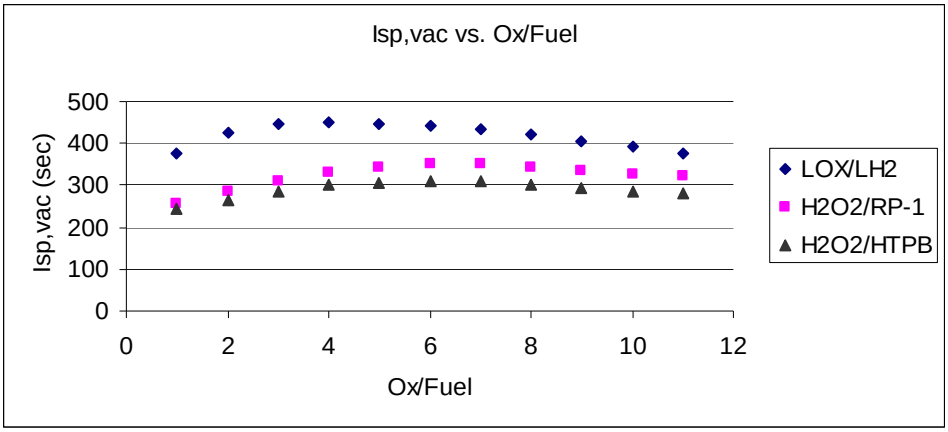

Fig. Section A.4.2.2.5.2.2: Vacuum Isp versus oxidizer to fuel ratio.
(Wilcox, Nicole)

While both specific impulse diagrams show the same optimum performance at the same oxidizer to fuel ratio, one can see in Fig. A.4.2.2.5.2.3 below that the optimum characteristic velocity occurs at a smaller oxidizer to fuel ratio.

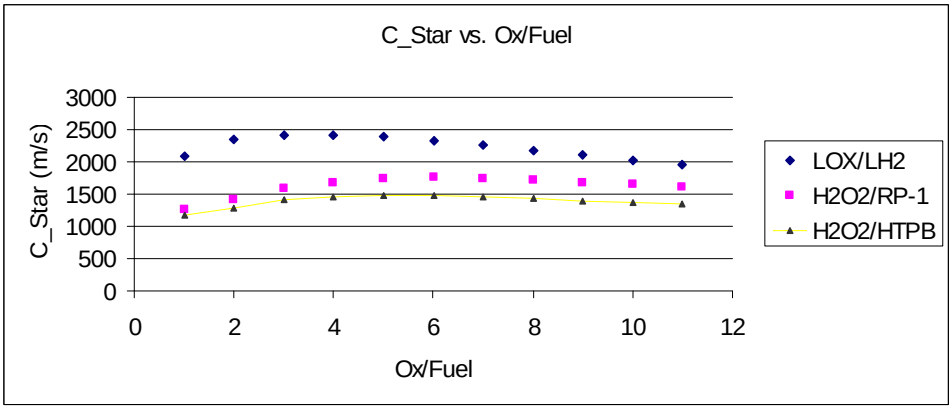

Fig. Section A.4.2.2.5.2.3: Characteristic velocity versus oxidizer to fuel ratio.
(Wilcox, Nicole)

Due to the slight difference and our reliance on specific impulse rather than characteristic velocity for performance, we decided to choose the optimization based on specific impulses. Both variables are representative of the engine performance regardless. However, a higher specific impulse fit our needs better.

When analyzing this data another observation was made that the specific impulses between hydrogen peroxide / RP-1 and hydrogen peroxide / HTPB had little variation from one another.

This small variation made us suspicious early on of the possibility that selecting a hybrid is more beneficial than selecting a storable. Our observation was later proven by the Model Analysis simulations. Mixture ratio analysis proves beneficial in understanding of the oxygen to fuel ratio, optimizing engine performance, and providing insight into future choice possibilities.

4.2.3 Basic Propulsion Equations

A main concern throughout the development of our project is the mass of our rocket. Mass is a directly tied to the overall cost of our launch system; as mass goes up so does the cost of the system. Therefore, we must take as many steps as possible to reduce the mass of our launch system as much as possible.

The basic equation for finding a rough estimate of a launch vehicle's mass is by using basic sizing equations. By knowing several pieces of information it is possible to determine the mass of our vehicle. Some of the required information is as follows:

- Required Velocity Change, more commonly referred to as DeltaV
- Mass of Payload (including other essential hardware, such as avionic packages)
- Specific Impulse of Propellant
- Inert Mass Fraction (amount of total mass that is not propellant)
- Number of Stages

These five main variables tend to be known, at least generally, by the designer at the start of design. We have values for each of these variables and therefore can proceed in sizing our launch vehicle. The first equation we will use will tell us the mass of propellant required to complete the mission.[1]

$$m_{prop} = \frac{m_{pay}\left[e^{\frac{\Delta V}{I_{sp}g_0}} - 1\right](1 - f_{inert})}{1 - f_{inert}e^{\frac{\Delta V}{I_{sp}g_0}}} \qquad \text{(A.4.2.3.1)}$$

Here m_{prop} is the mass of the propellant in kilograms, m_{pay} is the mass of the payload in kilograms, ΔV is the required velocity change in m/s, Isp is the specific impulse of the propellant in seconds, g_0 is the gravity constant in m/s^2, and f_{inert} is the inert mass fraction.

Since all of the variables in equation A.4.2.3.1 can be broken up into components based on which stage they are operating on we can find the required propellant mass for each leg of the mission. The amount of propellant mass required and the inert mass fraction can be combined to find the amount of inert mass required for each stage and payload mass. By using equation

A.4.2.3.2 we can find the amount of inert mass we may expect based on propellant mass and inert mass fraction.[1]

$$m_{inert} = \frac{f_{inert}}{(1 - f_{inert})m_{prop}} \qquad \text{(A.4.2.3.2)}$$

Combining the output from equations A.4.2.3.1 and A.4.2.3.2 with payload and avionics masses we can obtain the approximate total mass for each stage of the launch vehicle. Note that when sizing a multi-stage rocket the total weight of the upper stage will be the payload weight for the stage below it and so on down the rocket. From the data above and information about the propellants being used items such as volume and cost of propellant are determined.

These are the basic principles that we used to size our rocket throughout all stages of development. The sizing code based off of the equations in this section will be used extensively in Model Analysis to determine the exact specifications of our launch vehicle. Team members from the propulsion and structures groups will collaborate together using these equations, and others, to find the lowest cost feasible launch system possible.

Not only is mass another major concern, we also have problems with sizing the nozzle or finding the expansion ratio. If we miscalculate the nozzle's size, flow separation can occur, preventing our launch vehicle from obtaining enough thrust to launch. We know that expansion ratio is a function of the pressure ratio as shown in Eq. (A.4.2.3.1).[1]

$$\varepsilon = \frac{A_t}{A_e} = \left(\frac{\gamma+1}{2}\right)^{(1/(\gamma-1))} \left(\frac{Pe}{Pc}\right)^{1/\gamma} \sqrt{\frac{\gamma+1}{\gamma-1}\left[1 - \left(\frac{Pe}{Pc}\right)^{(\gamma-1)/\gamma}\right]} \qquad \text{(A.4.2.3.1)}$$

where Pe represents the exit pressure, Pc represents the chamber pressure and γ represents the specific heat ratio. However, we can calculate the expansion ratio using a range of pressure ratios associated with our propellants and the CEA code (explained further in Section A.4.2.2.5).

Next, we use sea level thrust Eqs. (A.4.2.3.2), (A.4.2.3.3) and (A.4.2.3.4) and the GLOW to find area of the throat at each stage. According to Humble, most launch vehicles have T/W ratios that range from 1.2 to 1.5 and the team uses a recommended value of 1.2.[1,2]

$$Avg\_T = 1.2 * GLOW * g \tag{A.4.2.3.2}$$

and

$$Avg\_T = 1.2 * (GLOW - stage\_mass(1)) * g \tag{A.4.2.3.3}$$

and

$$Avg\_T = 1.2 * (GLOW - stage\_mass(1) - stage\_mass(2)) * g \tag{A.4.2.3.4}$$

where g represents gravity and GLOW represents the gross lift-off weight. To correctly calculate thrust, we need to account for the loss of mass as our launch vehicle accelerates. Then using Eq. (A.4.2.3.5), we calculate throat area which then helps us to calculate exit area shown in Eq. (A.4.2.3.6).[4]

$$\begin{aligned} A_t = {} & (\text{Avg\_T})./ \\ & (\text{Pc}.*\gamma.*[((2./(\gamma\text{-}1)).*(2./(\gamma\text{+}1)).\hat{}((\gamma\text{+}1)./(\gamma\text{-}1))).*(1\text{-}((\text{Pc\_Pe}).\hat{} \\ & \text{-}1).\hat{}((\gamma\text{-}1)./(\gamma)))].\hat{}(0.5) \\ & + (((\text{Pc\_Pe}).\hat{}\text{-}1).*\text{Pc} - 2880).*e) \end{aligned} \tag{A.4.2.3.5}$$

where Pe represents exit pressure, Pc represents the chamber pressure, γ represents the specific heat ratio and Avg_T represents sea level thrust.

$$A_e = \varepsilon * A_t \tag{A.4.2.3.6}$$

where ε represents the expansion ratio and At is the throat area.

To find the engine mass, we assume that this value only consists of the masses of the nozzle (Eq. A.4.2.3.7) and of the injector (Eq. A.4.2.3.8).

$$m_{noz} = 125\left(\frac{m_{prop}}{5400}\right)^{\frac{2}{3}}\left(\frac{\varepsilon}{10}\right)^{\frac{1}{4}} \qquad \text{(A.4.2.3.7)}$$

and $$m_{inj} = (0.184) * m_{noz} \qquad \text{(A.4.2.3.8)}$$

where m_{prop} represents the mass of the propellant and ε represents the expansion ratio.

Knowing the expansion ratio and the areas of the nozzle, we can continue with calculating the other engine parameters such as mass flow, nozzle length, etc. Using these basic equations, the Trajectory and Structures groups can calculate their unknowns and continue to search for the lowest cost feasible launch system possible.

References

[1] Humble, R. W., Henry, G. N., Larson, W. J., "Rocket Fundamentals," *Space Propulsion Analysis and Design*, 1st ed., Vol. 1, McGraw-Hill, New York, NY, 1995, pp. 18, 214-217.

[2] Tsohas, John, AAE 450 class, West Lafayette, IN, 2/20/08.

[3] Sutton, G., P., Biblarz, O., "Solid Propellant Rocket Fundamentals," *Rocket Propulsion Elements,* 7th ed., Vol. 1, Wiley, New York, NY, 2001, pp. 63.

A.4.2.4 Pressurization Systems

A.4.2.4.1 Pressure Fed

Our chosen method of pressurizing the propellant tanks is a pressure – fed system. Propellant feed systems account for a large portion of the mass and cost of an engine for a launch vehicle. Historically, smaller rockets tend to use pressure fed propellant feed systems due to their simplicity and cost.[1] Pressure-fed systems require an extra tank and gaseous pressurant. This adds more mass but is necessary for the fuel to overcome the adverse pressure gradient and enter the chamber.

Pressure-fed systems require the selection of a pressurant and two options commonly used and closely investigated are nitrogen and helium. Nitrogen is less expensive at $0.50/kg than helium at $20/kg.[2] Helium also has the disadvantage of being a very small diatomic molecule. Should our tanks be constructed of a very porous material, the helium molecules could leak through the material and render the feed system useless. Even with a small amount leakage, additional helium would be stored in the tanks for balloon launch due to the long ascent. Some materials are capable of containing helium, but using these materials and specially manufacturing all tanks to hold helium would significantly increase costs. Pressurant will eventually enter all tanks therefore all tanks must be designed to contain helium as well as fuel or oxidizer. Our conclusion is to use nitrogen because of pricing, molecule size, and more frequent use in launching history.

To calculate the proper mass of the pressurant first we must know the final temperature of the pressurant in the tanks. For this we assume isentropic expansion with constant γ and use Eq. (A.4.2.4.1).

$$T_f = T_i\left(\frac{p_f}{p_i}\right)^{\frac{\gamma-1}{\gamma}} \qquad \text{(A.4.2.4.1)}$$

where T_f is the final temperature, T_i is the initial temperature of the propellant, p_f is the final pressure of the pressurant, p_i is the initial pressure of the propellant, and γ is the ratio of specific heats.

The initial temperature is considered ambient temperature, the final pressure must be greater than the chamber pressure, the initial pressure is arbitrarily chosen to minimize the added inert mass but still maintain a pressure high enough to keep temperatures reasonable. After the final temperature is found, one can use Eq. (A.4.2.4.2) to find the mass of the propellant:

$$m_{press} = \frac{V_{press} p_f}{R T_f} \qquad \text{(A.4.2.4.2)}$$

where T_f is the final temperature, p_f is the final pressure of the pressurant, m_{press} is the mass of pressurant required, and V_{press} is the final volume that the pressurant must fill at the final pressure.

To find the volume of the tank that the pressurant will initially be held in, one can simply rearrange the previous equation and use initial values for pressure and temperature rather than final. In Eq. (A.4.2.4.2), the initial volume is simply the volume of the pressurant tank itself, but the final volume is the volume of the pressurant tank as well as all other liquid propellant tanks, fuel and oxidizer. An iterative solution was not used due to the assumption that the pressurant volume would be low in comparison with the oxidizer and fuel tanks. This proved true as in all cases the volume added by the pressurant tank was no more than 2.86% of the summed tank volume. Using the previous formulae, the below values were found for all three vehicles.

Table A.9.2.3.1 Pressurant Mass and Cost per Launch Vehicle [a]

Payload	Pressurant Mass (kg)	Pressurant Volume (m^3)
200 g	59.0	0.1158
1 kg	38.2	0.0751
5 kg	166.3	0.3266

[a] numbers based on initial pressure of 12 MPa

In our final design, pressurant is only located in the first stage of each rocket due to the use of hybrid engines for those stages. A liquid injection thrust vector control (LITVC) is located on the second stage, but consists of a self-pressurized tank. Spin stabilization is used on the third stage so neither pressurant or LITVC is necessary. Pressurant only accounts for a small portion of the total mass of the first stage in each rocket, but without pressurant, the oxidizer would simply not feed into the chamber at all due to an adverse pressure gradient because of the high chamber pressure.

References

[1] Humble, R. W., Henry, G. N., Larson, W. J., Space Propulsion Analysis and Design, McGraw-Hill, New York, NY, 1995.

[2] "Missile Fuels Standard Prices Effective Oct 1, 2007.", Defense Energy Support Center, Fort Belvoir, Virginia, July 2007. [http://www.desc.dla.mil/DCM/Files/MFSPFY08_071107.pdf. Accessed 1/15/08.]

[3] Sutton, G., Biblarz, O., Rocket Propulsion Elements, John Wiley & Sons, Inc., New York, NY, 2001.

A.4.2.4.2 Pump – fed Propellant System

When selecting a propellant feed system there are many factors to consider. Our concern for this project was mainly cost which automatically rendered the use of a pump-fed system infeasible. However, it is important to understand the reasons why this was simply not possible.

Historically, pump-fed systems are used on larger launch vehicles due to the need to reduce inert mass.[1] When using a pressure-fed system, the tanks must be capable of withstanding large pressures and pressure variances. Also, the tanks only need to withstand the g loadings.[2] The turbopump will pressurize the propellant extracting the propellant from the tank and forcing it into the chamber for combustion.

While pump-fed systems allow for less structure, using this system increases complexity of the launch vehicle. This complexity is translated into cost. Some of our research was estimating the cost of a turbopump for the amount of thrust we required. The smallest turbopump we found was capable of pumping propellant to an engine that created 89,000 N of thrust with the following costs:

Table A.9.2.3.1 Cost of Turbopumps [3]

Number of Turbopumps Purchased	Minimum Cost per Pump	Maximum Cost per Pump
3-15	$300,000	$500,000
15-20	$100,000	$150,000

Because companies specialize turbopumps to the customers needs, Barber-Nichols could only give us a range of estimated costs for the turbopumps. In addition, research and development of the turbopump needed would cost 2-5 million dollars.[3] Also, turbopumps for launch vehicles become more expensive as they become smaller.[3] For a small launch vehicle on a budget these factors simply do not allow us to chose a pump-fed system.

References

[1] Humble, R. W., Henry, G. N., Larson, W. J., Space Propulsion Analysis and Design, McGraw-Hill, New York, NY, 1995.

[2] Sutton, G., Biblarz, O., Rocket Propulsion Elements, John Wiley & Sons, Inc., New York, NY, 2001.

[3] Personal Interview., Sales manage. Barber-Nichols, Inc., Arvada, Colorado, 2/13/08.

A.4.2.4.3 Injectors

For this project, we black-box many of the components of the engine, including the injector since we only focus on top-level design. However, we use this section to discuss injectors in case of further in-depth analysis of our launch vehicle.

We looked at many different injector formations and decided which type of injection method worked best for our liquid propellants. For our cryogenic liquid propellant, we chose liquid oxygen (LOX) and liquid hydrogen (LH_2). For our storable propellant, we chose hydrogen peroxide (H_2O_2) and RP-1.

After studying many different types of injection methods we decided to use an injector with a concentric tube injector with possible liquid swirl injection for our propellant choices. This means that the oxidizer is fed through a center tube and the fuel is fed in a separate concentric tube surrounding the oxidizer. Fig. A.4.2.4.3.1 show this schematic. The oxidizer is fed through the center while the fuel is surrounding the oxidizer tube in this cross section schematic.

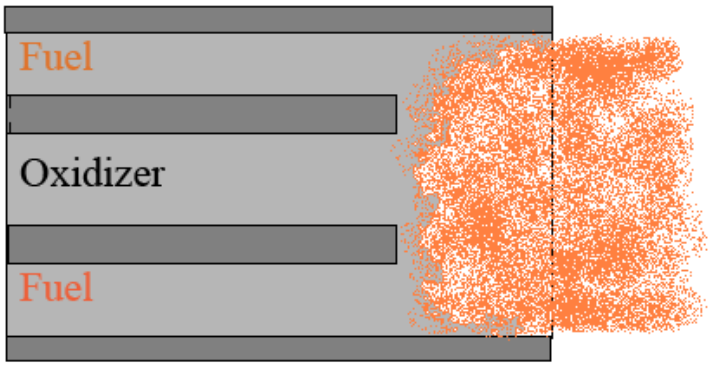

Figure A.4.2.4.3.1: Concentric tube injector for liquid fuels.
(Ricky Hinton)

This concentric tube design has good stability characteristics for our cryogenic liquid propellants. For example, the Space Shuttle main engine uses this injection method using LOX and LH_2.[1] For our storable propellants, we need a slightly better mixing so we can use the same concentric design, but we introduce a swirl to the liquid fuel stream. The liquid fuel swirls around in its concentric tube so when introduced to the oxidizer, a better mixing takes place.

In hybrid rocket motors, these injector plates feed oxidizer into the chamber to help atomize the propellant. Typical required pressure drops range from 20% to 30 %.[2] In the code, **stage**, we assume a pressure drop of 20%.

The design process of an injector, especially of liquid propellant injectors optimize many of the design parameters and many of the physical processes of the injector that occur simultaneously. For hybrid rocket motors, there exist two basic designs to consider: one that directly injects oxidizer down the port and another design that injects oxidizer into a precombustion chamber where the precombustion chamber gasifies and heats the oxidizer before it flows down the port. In either case, the oxidizer needs to go down the port to react with the propellant.
In early works, smaller motors with single ports use injectors that inject oxidizer directly down the port. Larger motors with multiple ports use injectors that inject into a precombustor. Larger motors use individual injectors, but this arrangement has a disadvantage if the ignition requires a hypergolic fuel. If so, then each injector would need its own means of injecting fuel. However, these individual injectors give high combustion efficiencies of 91-93% of equilibrium flow prediction.[2]

For our choice of oxidizer, H_2O_2, we consider impinging-like type of injectors. “Like” injectors use two oxidizers or two fuels. If we choose an injector that injects oxidizer into a precombustion chamber, then we must consider the more conventional liquid injectors to provide a uniform spray using injector types such as the showerhead, impinging jets, splash plates and swirl sprays. We also have to consider a length-to diameter (L/D) so the oxidizer has enough time to vaporize. Typical L/D of the precombustor area is about 0.5.[2]
For our final design, none of our stages uses liquid engines so we did not develop this type of injector design further. This section may provide an insight for future design changes if a liquid

engine ever is needed for any of these launch vehicles. As we stated before, we do not have any detailed analysis on hybrid injectors because we only focus on top-level design.

References

[1]AAE 439 class notes fall 2007. Professor Hrbud. Injectors: supplementary handout. pg. Ch6-39a.

[2]Humble, R. W., Henry, G. N., Larson, W. J., "Hybrid Rocket Propulsion Systems," Space Propulsion Analysis and Design, 1st ed., Vol. 1, McGraw-Hill, New York, NY, 1995, pp. 366, 424-425.

A.4.2.5 Nozzle

When designing the nozzles for our rocket engines we looked at the two basic types of nozzles that are used today, conical and Bell nozzles. There are other types of nozzles besides just these two such as: Plug nozzles, extendible nozzles, etc. However, these types of nozzles were not considered for the final design of our launch vehicle because in many cases they are still in development. We decided we would go with a proven design with plenty of historical data to support it. When we designed the nozzle we kept in mind both the pros and cons to both the conical and Bell shaped nozzles.

The conical nozzle is simply a cone shape described by the cone's half angle as viewed from the side. For instance if the nozzle is described as a 12 degree conical nozzle this means that from the centerline of the nozzle to the inside wall there is a 12 degree angle. This type of nozzle is seen historically and is typical for solid and hybrid rocket engines. Some of the advantages of a conical nozzle are its simple cone shape for design, and it contains no inflection as the propellants are expelled from the combustion chamber. This lack of inflection means that the nozzle is a straight line coming out of the throat to the exit. This inflection angle can be seen in Fig. 4.2.5.1 in respect to a Bell nozzle shape. This lack of inflection is critical for solid and hybrid engines because these types of engines usually have some pieces of solid propellant expelled all the way out of the nozzle. Therefore, a conical nozzle is desired for solid and hybrid propellant types due to the lack of inflection.

One of the disadvantages of a conical nozzle is the fact that there is a significantly more divergence loss at the exit. The propellant flow strives to be completely parallel to the centerline of the nozzle as it exits. Since the exit angle of a conical nozzle is the same as the cone angle, the flow exits at not parallel but rather at the cone angle. When there is an angle at the exit the flow experiences a divergence loss which causes energy loss and in turn a loss of nozzle efficiency. With a conical nozzle the exit angle is large and therefore the divergence loss is maximized. Another disadvantage is a conical nozzle contains more material and therefore mass than a Bell nozzle of the same design. In general for a design, the more massive the launch vehicle is the more expensive it will be. These factors are all some of the downfalls when using a conical nozzle design.

The next part in our design was to consider a Bell nozzle. Bell nozzles are based off of a conical nozzle design but are more efficient and more compact than a conical nozzle. Some of the advantages of a Bell nozzle are that it reduces the divergence loss at the exit, it is less massive, and in turn more efficient than a conical nozzle. The divergence loss at the exit of a bell nozzle is significantly less than that for a conical nozzle of the same design. The exit angle for a 15 degree conical nozzle is 15 degrees, while the exit angle of a Bell nozzle with the same exit diameter is only 8.5 degrees. This can be seen in Fig. 4.2.5.1 on the next page. Also the bell nozzle is shorter and has less mass than the conical nozzle because it is more compact. These characteristics make a Bell nozzle much more efficient than a straight conical nozzle.

However, a disadvantage to a Bell nozzle is it can only be applicable for liquid rocket engines. This is because the solid propellants expel particles which would deteriorate a Bell nozzle. When applied to a Bell nozzle shape these "chunks" of propellant are forced into the walls of the nozzle and can cause significant deterioration. This happens because the Bell nozzle has some inflection to its shape as was mentioned earlier. For this reason this bell nozzle was considered in early designs when a liquid propellant system was still feasible. The final designs for our launch vehicles did not include any liquid engines, and therefore the Bell nozzle was not used for the final design.

Figure 4.2.5.1 below shows how our Bell nozzle was designed. The first step is to choose a conical shape and a corresponding half angle. For our initial design of a Bell nozzle we chose arbitrarily a 15 degree half angle. Using the MAT outputs which give us an expansion ratio and throat area the dimensions of the exit diameter could be determined. This shape has a finite length (L) as a conical nozzle as shown in the bottom half of Fig. 4.2.5.1. We decided to use an 80% Bell Contour for our design.[1] Bell Nozzles historically work the best when they are between 75%-85% so we decided to go with the average of these values and used 80%. An 80% Bell contour means that the length from throat to exit of the Bell nozzle is 80% of the original length (L) for a conical nozzle. Since the throat diameter and exit diameter are known a parabolic shape is constructed to join the throat to the exit in this reduced nozzle length (L). The resulting shape is an 80% Bell contour nozzle.

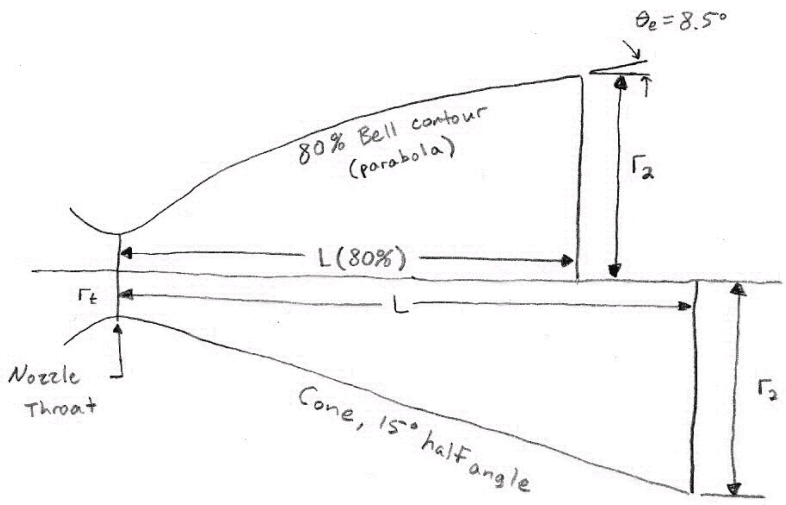

Figure 4.2.5.1: Bell Nozzle design based on conical nozzle shape
(Hinton, Ricky)

The CAD models were done for both the conical and Bell nozzles. However with the final design for Project Bellerophon only our conical nozzle designed for solid and hybrid proppelants were included for the final models. CAD drawings were completed in CATIA.

The conical nozzle CAD model was designed by first making a profile of the cone half angle. From the MAT outputs the exit diameter and expansion ratio were known values. Using this expansion ratio (ε) and the exit area (A_e) based on the exit diameter, the throat area (A_t) and thus throat diameter could be determined using Eq. A.4.2.5.1 below.

$$\varepsilon = \frac{A_e}{A_t} \qquad \text{(Equation A.4.2.5.1)}$$

The profile view was then rotated along the centerline in order to make a solid nozzle shape. The nozzle shape was then shelled out in order to make the nozzle. The finished CAD model can be seen in Fig. A.4.2.5.2 below.

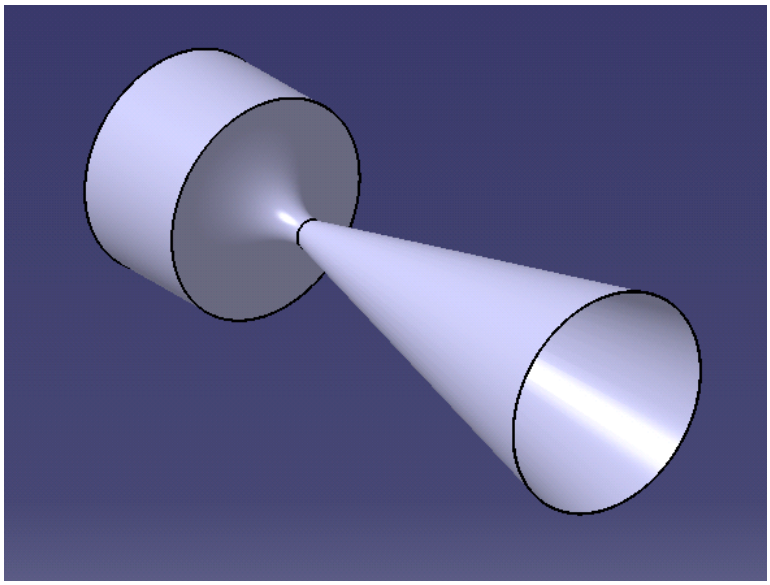

Figure A.4.2.5.2: Conical Nozzle CAD
(Hinton, Ricky)

All of the conical nozzles that were used for our final design are represented in our final CAD models. All of the nozzles have the shape shown above, and only differ in the throat and exit diameters. As I mentioned earlier the values for exit area were obtained from the outputs to our MAT codes. From these values the exit diameter could be calculated. The expansion ratio for all of our engines was constant at $\varepsilon = 60$. This is because for our final design the first engine would be ignited at an altitude of approximately 30,000 km. At this altitude the ambient pressure of the atmosphere is already very low. All of the final nozzles were therefore modeled after upper stage engines. Using this expansion ratio the throat area and throat diameters could be calculated. Table A.4.2.5.1 below shows all of the values used for the final nozzles. These variables are: throat diameter D_t , exit diameter D_e, throat area A_t, exit area A_e, and stage diameter D_{stage}. The stage diameter is included to give a reference of how large the nozzle exit is in comparison to the entire staged vehicle. Each launch vehicle is represented in this table.

Table A.4.2.5.1: Values of nozzle parameters.

Launch Vehicle	D_t (m)	D_e (m)	A_t (m^2)	A_e (m^2)	D_{stage} (m)
5 kg					
Stage 1	0.159	1.235	0.0200	1.198	1.839
Stage 2	0.00385	0.299	0.00117	0.070	0.817
Stage 3	0.00798	0.0618	0.00005	0.003	0.275
1 kg					
Stage 1	0.085	0.660	0.0057	0.342	1.126
Stage 2	0.024	0.189	0.000467	0.028	0.567
Stage 3	0.008	0.062	0.00005	0.003	0.290
200 g					
Stage 1	0.107	0.831	0.00905	0.543	1.302
Stage 2	0.029	0.226	0.000667	0.04	0.674
Stage 3	0.008	0.062	0.00005	0.003	0.272

To give a relative size comparison all of the nozzles can be seen in the same figure next to each other in Fig. A.4.2.5.3. This figure represents the nozzles for all three stages of the 5 kg case. As you can see the nozzles get significantly smaller as they go from stage one to stage three. The diameter values for the given 5 kilogram stage nozzles can be found in the table above. All of the final nozzles have similar sizes in respect to the nozzles of each of their stages.

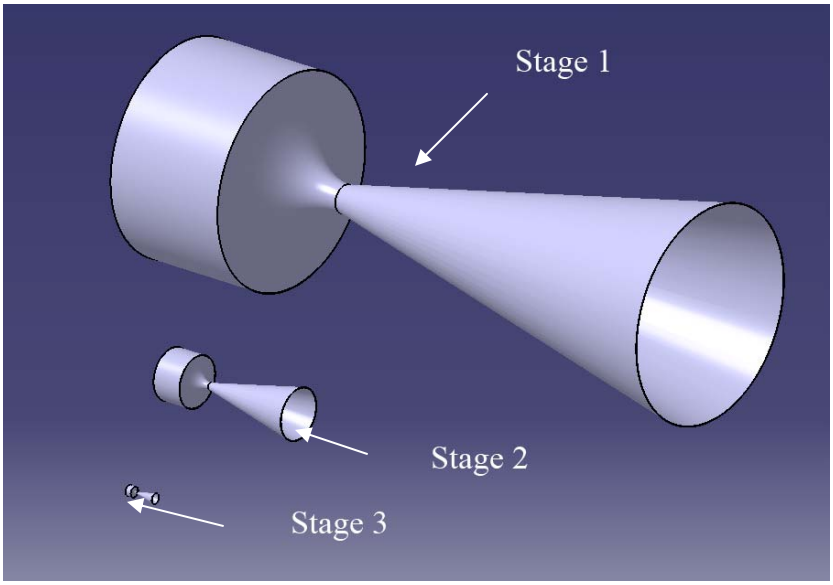

Figure A.4.2.5.3: All three stage nozzles for 5 kg case.

(Hinton, Ricky)

One point for us to consider is the following: Is a nozzle with throat diameter as small as 8 millimeters a feasible design? This is the case for the stage three nozzles for both the one kilogram and two hundred gram launch vehicles. After talking to our project advisor, Mr. John Tsohas, he informed the team that a throat diameter this small was in fact feasible. However the problem is when a throat diameter gets this small the losses that the flow undergoes at the throat are substantially increased. The engine may not perform as it is expected to. This is definitely a big issue that a subsequent design team would have to address, but for our team's scope and time constraint we were not able to obtain a final answer on.

References

[1]AAE 439 class notes fall 2007. Professor Hrbud. Contour Design. pg. Ch4-69 – Ch4-70

A.4.2.6 Attitude Control

For attitude control of the launch vehicles, two separate systems were investigated. The first system was a gimbaling nozzle, and the second was a liquid injection thrust vector control (LITVC) system. Each system had its pros and cons but the LITVC system was finally chosen.

A.4.2.6.1 Gimbaling

When investigating the gimbaled nozzle, several different historical configurations were investigated. Only the first and second stages are to be outfitted with thrust vector control since the third stage is spin stabilized. The first stage has a hybrid engine and the second stage has a solid engine. These two types of engines greatly limit the gimbaling abilities due to the design and structure of the engines. For a gimbaling system with liquid engines, the entire engine with the powerhead can be moved as one solid piece, but this cannot be done with either a hybrid or solid engine. Both of these engines have a solid, single piece for a nozzle where the exhaust flows through from a burning solid upstream. Due to this solid structure and exhaust flow, the nozzle would need a flexible seal in which the nozzle end can rotate while still holding a seal that will prevent the hot exhaust gases from escaping at those points. Several studies were looked at about gimbaled nozzles including a technical report for NASA which specifically dealt with the flex seal nozzle.[1] Due to the complexity of the parts within the nozzle and the increased cost of the thrust vectoring due to manufacturing, this option was not used.

A.4.2.6.2 LITVC

The final thrust vector control system that was investigated was liquid injection thrust vector control (LITVC). This system looks very attractive for our application due to the low manufacturing cost and the moderate complexity of the parts vs. a gimbaled nozzle. The main parts of the LITVC system are the valves, injectors, and storage tanks.

The first stage is going to be a hybrid engine with H_2O_2 as the oxidizer. Since a tank with H_2O_2 was needed for the main engine, we decided to tap off from the main tank in order to use H_2O_2 as the LITVC injectant. H_2O_2 is a very desirable liquid due to its stable room temperature form and low handling costs. Once injected into the main flow stream within the rocket nozzle, the H_2O_2 instantly decomposes due to the heat and pressures within the nozzle. When the H_2O_2 decomposes, it greatly expands which allows for a larger side force to be generated giving the desired thrusting capabilities for control. Since a tap off of the main tank is used, the extra weight associated with the first stage includes the extra H_2O_2 needed for LITVC as well as the slightly larger volume of the main tank in order to account for the extra H_2O_2.

The LITVC system for the second stage is very similar to the first stage's only that there is no H_2O_2 tank on the stage. A tank that is curved will be added underneath the second stage solid tanks in a position curving around the nozzle in order to minimize space. The tank will be pressurized to a set pressure before launch and will require no additional pressurant in order to achieve the desired mass flow rate to the injectors. The rest of the LITVC system will be the same as with the first stage, except that the injectors, valves, and venturis will need to be smaller in order to lower the thrust and the flow rate of H_2O_2 entering the nozzle.

The LITVC system for each stage and payload will vary depending on the size of the stage and the amount of side thrust needed. Figure A.4.6.2.1 provides a guide to which the mass flow rate of propellant into the nozzle can be calculated.

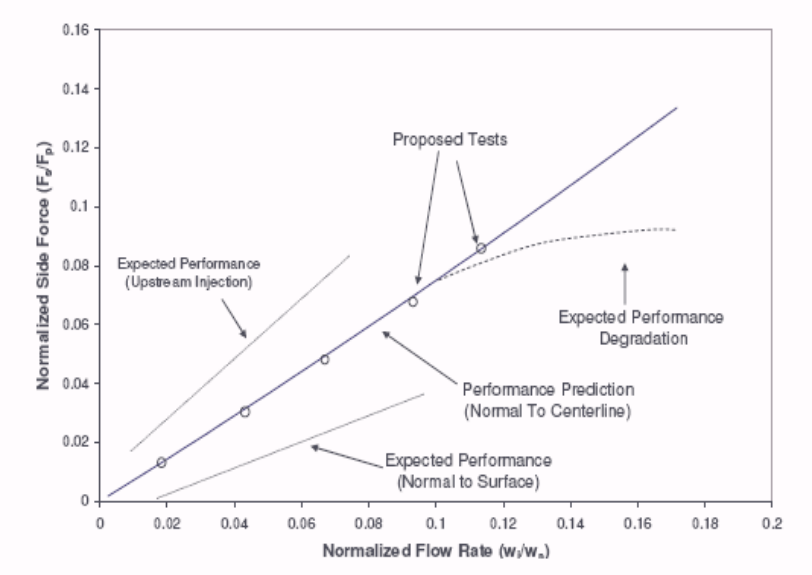

Fig. A.4.6.2.1 Side Force over Primary Force vs. Side Flow Rate over Primary Flow Rate for LITVC[2]

When the optimization (MAT) codes are run, the primary thrust and mass flow rates are calculated and output. From this, a normalized side force of 0.08 is assumed since the primary thrust is relatively low. This higher normalized side force will allow a higher side thrust and should allow more control capability. Once the normalize side force of 0.08 is used, Fig. A.4.6.2.1 is used to find the normalized flow rate which comes out to 0.09. With this number and the primary mass flow rate output by the MAT codes, the side mass flow rate can be calculated using Eq. (A.4.6.2.1).

$$\dot{m}_s = \dot{m}_p * 0.09 \qquad \text{(A.4.6.2.1)}$$

where $\dot{m}_s$ is the mass flow rate of the LITVC injector and $\dot{m}_p$ is the mass flow rate of the main engine. With the mass flow rate, the amount of propellant is then calculated. The D&C group set a LITVC thrusting time of one-third burn time of the main engine as a very conservative estimation using their analysis. With the calculated LITVC mass flow rate, injection time, and density of the H2O2, the volume of propellant was calculated using Eq. (A.4.6.2.2)

$$V = \dot{m}_s * t_i * \rho \qquad \text{(A.4.6.2.2)}$$

where V is the volume of the propellant, $\dot{m}_s$ is the mass flow rate of the LITVC injectant, t_i is the time of injection, and ρ is the density of the injectant. The volume calculated can then be used to add to the first stage propellant or to determine the tank size of the second stage LITVC system.

References

[1] Ciepluch, Carl, "Technology for Low Cost Solid Rocket Boosters," NASA TM X-67912, November 1971.

[2] Case IV, E. G., "Preliminary Design of a Hybrid Rocket Liquid Injection Thrust Vector Control System," *AIAA Paper*, No. 2008-1420, January 2008

A.4.2.7 Engine Performance

A.4.2.7.1 Liquids

Propellant combustion theory varies between different types of propellant. This is evident in appearance of thrust-time curves. Liquid rocket engines are typically used for large shuttle launches because they can throttle in real-time and offer start-stop control. These engines provide relatively constant thrust profiles similar to Fig. A.4.2.7.1.1 where T is thrust. Douglas H. May created this plot to show the general trend of liquid performance of thrust-time curves.

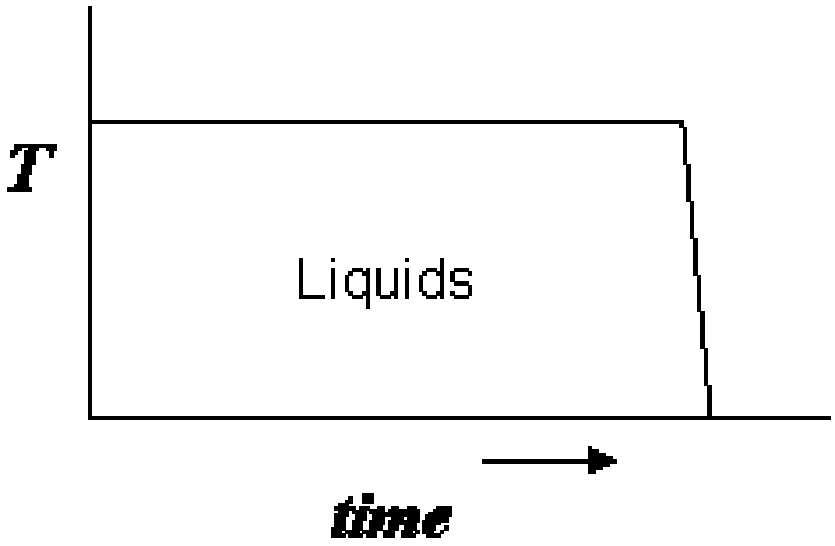

Fig. A.4.2.6.1.1 Thrust-time curve of burned liquid propellant.
(Douglas H. May)[1]

We assumed constant thrust for our calculations where total impulse is equal to the area under the curve of thrust versus time. Eq. (A.4.2.7.1.1) shows this relationship.[2]

$$I_t = \int_0^t T\, dt \qquad \text{(A.4.2.7.1.1)}$$

where I_t is total impulse, T is thrust and t is time. We made this assumption because of negligible start and stop transients. Additionally, in liquid propellant combustion theory, there exist little oscillations in the thrust curve profile due to nozzles with fixed geometry with rigid walls and feed systems which provide a steady flow of liquid propellant.

As stated before, combustion theory varies between different propellants. Hybrid and solid combustion theories greatly differ from liquid combustion theory.

References

[1] May, Douglas, H., "Rocket Science," *Orbital Mechanics*, DRD Corporation, Saddle-Brooke, Arizona, 2005. [http://www.orbitmechanics.com/Rocket_Science.html. Accessed 2/23/08.]

[2] Sutton, G., P., Biblarz, O., "Definitions and Fundamentals," *Rocket Propulsion Elements,* 7th ed., Vol. 1, Wiley, New York, NY, 2001, pp. 27.

A.4.2.7.2 Hybrids

We look at hybrid rocket engines because they have several important advantages: they are safe because the fuel and oxidizer are stored separately, they are simpler than liquid bipropellant systems, they are insensitive to defects in the grain, and they have low operational costs. Hybrids can be throttled by simply reducing the oxidizer flow. While not used in our design, throttling provides fine-tuning ability for trajectory. Hybrid rocket engines only significant disadvantage is that their burning rate is usually about ten times smaller than the burning rate in a solid rocket motor. This lower burning rate means that a much larger burning area is required for the same amount of thrust, requiring the use of multi-ports and increasing the cost.

The following is an outline of the method that we use to analyze hybrid rocket engines. The chamber pressure, P_c, is a function of the mass flow rate out of the chamber, $\dot{m}_{out}$, the throat area, A_t, and the characteristic velocity of the propellant, c^*.

$$P_c = \frac{\dot{m}_{out} A_t}{c^*} \qquad \text{(A.4.2.7.2.1)}$$

The mass flow rate of the oxidizer, $\dot{m}_{ox}$, is assumed to be held constant. The fuel mass flow rate is proportional to the fuel density, the burning rate, and the burn area.

$$\dot{m}_f = \rho_f r A_b \qquad \text{(A.4.2.7.2.2)}$$

where ρ_f is the fuel density, r is the burning rate, and A_b is the burn surface area. The total mass flow rate is then the sum of the oxidizer and fuel mass flow rates.

$$\dot{m}_{out} = \dot{m}_{ox} + \dot{m}_f \qquad \text{(A.4.2.7.2.3)}$$

where $\dot{m}_{out}$ is the total mass flow rate, $\dot{m}_{os}$ is the oxidizer mass flow rate, and $\dot{m}_f$ is the fuel mass flow rate.

This analysis assumes that the burning rate is a function of the mass flux, G, and two experimental parameters.

$$r = aG^n \tag{A.4.2.7.2.4}$$

where a is the burning rate coefficient, n is the burning rate exponent, and G is the mass flux. Mass flux is defined in Eq. (A.4.2.7.2.5).

$$G = \frac{\dot{m}_{out}}{A_p} \tag{A.4.2.7.2.5}$$

where $\dot{m}_{out}$ is the total mass flow rate and A_p is the port area. The port area is the area in which combustion occurs, measured in a plane perpendicular to the engine's axis of symmetry and is shown in Figure A.4.2.7.2.1. The total port area is simply the sum of the single port areas.

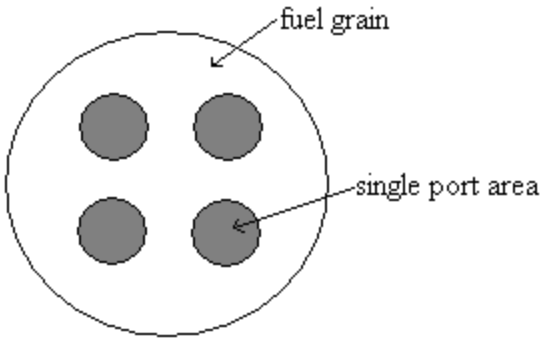

Fig. A.4.2.7.2.1: Top-down view of hybrid fuel grain.
(John Beasley)

The numerical calculations to determine chamber pressure requires an iterative process because *r* and $\dot{m}_f$ are functions of each other. The code **Hybrid.m** uses the following procedure to determine $\dot{m}_f$. First, a burn step size, Δw, is set. The burn area and port area for the given

geometry are then found by **Hybrid_Area.m**. For a given step, a value for $\dot{m}_f$ is guessed. Then, Eqs. (A.4.2.7.2.3) and (A.4.2.7.2.5) are used to find a value for G. Next, Eq. (A.4.2.7.2.4) is applied to find r. A new $\dot{m}_f$ is calculated using Eq. (A.4.2.7.2.2). This new value is compared to the initial guess. If the difference is less than some tolerance, the current $\dot{m}_f$ value is used as the guess for the next step. Otherwise, the current $\dot{m}_f$ is used as the starting point for another iteration.

The second part of the **Hybrid.m** code finds the chamber pressure, P_c. The chamber pressure is a function of the characteristic velocity, c^* and the mixture ratio, ϕ. The characteristic velocity is an output of the thermochemistry code. The mixture ratio is defined as the following:

$$\phi = \frac{\dot{m}_{ox}}{\dot{m}_f} \tag{A.4.2.7.2.6}$$

where $\dot{m}_{ox}$ is the oxidizer mass flow rate and $\dot{m}_f$ is the fuel mass flow rate. The code guesses a value for the chamber pressure, **cstar_lookup.m** then takes the chamber pressure and mixture ratio as inputs and outputs a value for the characteristic velocity based on a user-generated lookup table. **Hybrid.m** then calculates a new chamber pressure using Eq. (A.4.2.7.2.7).

$$P_c = \frac{\dot{m}_{out} c^*}{A_t} \tag{A.4.2.7.2.7}$$

where $\dot{m}_{out}$ is the total mass flow rate, c^* is the characteristic velocity, and A_t is the throat area. If the difference between the new chamber pressure and the chamber pressure guess is smaller than the tolerance, the next iteration begins with the chamber pressure guess equal to the chamber pressure from the previous iteration. If not, the procedure updates the chamber pressure and tries again.

Finally, the time and thrust level at each step are compute using Eqs. (A.4.2.7.2.8) and (A.4.2.7.2.9).

$$t = t_{i-1} + \frac{\Delta w}{r} \qquad \text{(A.4.2.7.2.8)}$$

where t is the time, t_{i-1} is the time at the previous step, Δw is the burn step size, and r is the burning rate.

$$F = c_f P_c A_t \qquad \text{(A.4.2.7.2.9)}$$

where F is the thrust, c_f is the ideal thrust coefficient, P_c is the chamber pressure, and A_t is the throat area.

Figure A.4.2.7.2.2 shows the initial geometry that was used to test the code, **Hybrid**, and Table A.4.2.7.2.1 lists the geometry values. The resulting thrusts, chamber pressures, and mass flow rates are shown as functions of time in Figs. A.4.2.7.2.3, A.4.2.7.2.4, and A.4.2.7.2.5, respectively. Table A.4.2.7.2.2 shows the values for the other parameters.

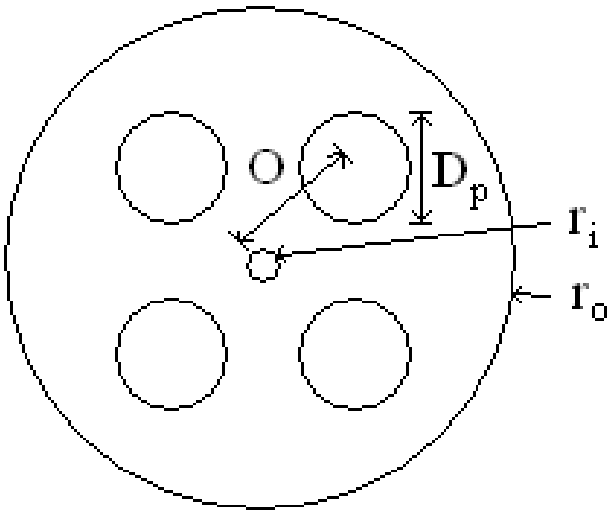

Figure A.4.2.7.2.2: Initial geometry used to test **Hybrid**.
(John Beasley)

Table A.4.2.7.2.1 Initial Geometry Values Used To Test **Hybrid**

Variable	Value	Units
D_p	1.375	m
r_i	0.29	m
r_o	2.375	m
O	1.238	m

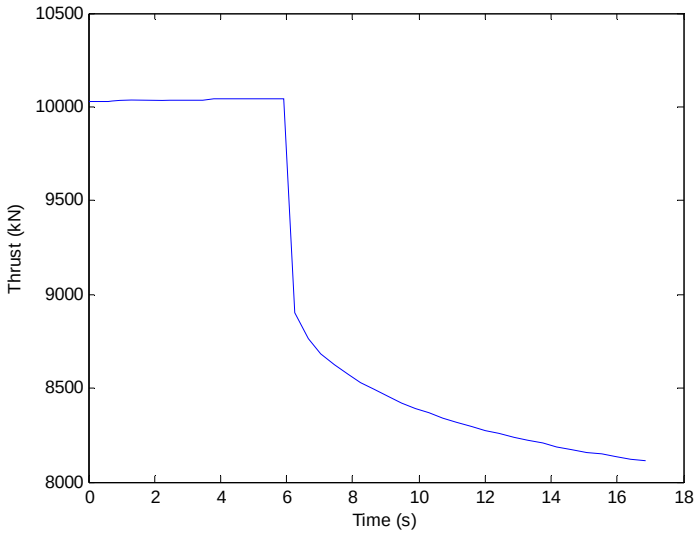

Figure A.4.2.7.2.3: Thrust profile for test geometry.

(John Beasley)

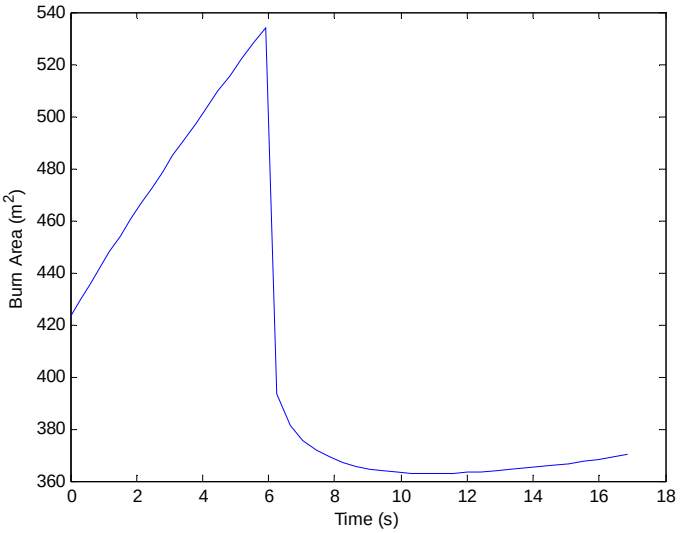

Figure A.4.2.7.2.4: Burn area profile for test geometry.

(John Beasley)

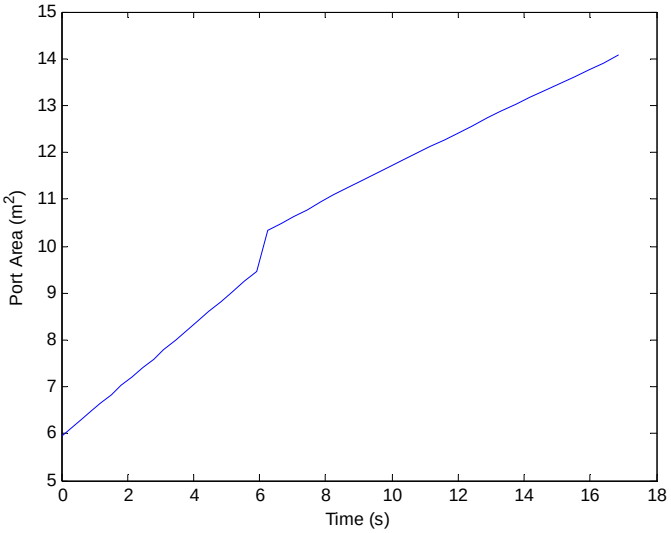

Figure A.4.2.7.2.5: Port area profile for test geometry.

(John Beasley)

Table A.4.2.7.2.2 Parameters Used To Test **Hybrid**

Variable	Value	Units
a	0.041	$\left(\frac{m^2 s}{kg}\right)^{0.49} \frac{m}{s}$
n	0.49	--
A_t	5	m^2
ρ_f	966	$\frac{kg}{m^3}$
$\dot{m}_{ox}$	3.6	$\frac{kg}{s}$
c_f	1.7	--
Δw	0.01	m

The next step would have been to integrate this code into the main design code. However, we decided to assume constant vacuum thrust to reduce the code runtime. At this point, work was stopped on hybrid rocket performance.

If more time were to be spent on this design project, there are several things that should be done in this area. First, a new burning rate correlation that takes into account position effects should be included. Also, the geometry should be made self-optimizing. Currently, the geometry must be input manually and is static. To speed optimization, the code should be able to take parameters such as stage length, stage diameter, maximum chamber pressure, and desired initial thrust and modify the initial geometry to fit the required performance. Finally, a thermochemistry code should be substituted for the characteristic velocity look-up table to improve accuracy.

A.4.2.7.2: Solids

We look at solid rocket motor systems because they have many advantages: simple and cheap compared to other systems, higher propellant mass fractions, higher thrust, and higher propellant densities than similarly sized systems. Some disadvantages include no provision for active throttling, testing difficulties, and low I_{sp}. The first two disadvantages are moot for this feasibility study: our simulator has no provision for throttling and our testing analysis has no costs associated with it.

The first and most difficult parameter that needs to be determined is the propellant burning rate, r. It describes the linear rate at which the propellant surface recedes.

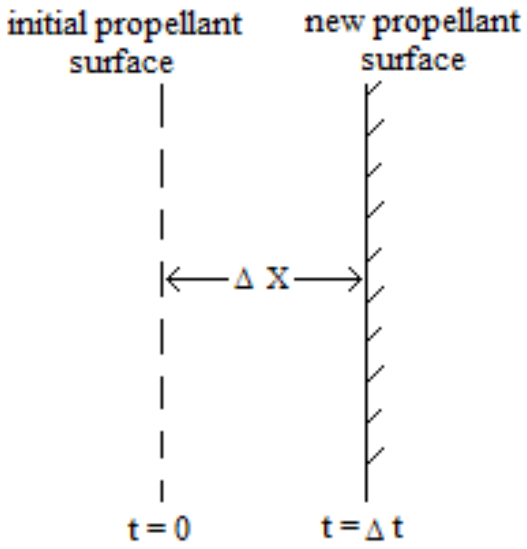

Fig. A.4.2.7.3.1: Diagram of burning rate definition.
(John Beasley)

The burning rate, as seen in Fig. A.4.2.7.3.1, is defined below.

$$r = \lim_{\Delta t \to 0} \frac{\Delta x}{\Delta t} \qquad \text{(A.4.2.7.3.1)}$$

where r is the burning rate, Δx is the infinitesimal burn distance, and Δt is the infinitesimal time. Burning rate is proportional to pressure. Propellant samples are burned at various pressures and the results are plotted on a log-log scale.

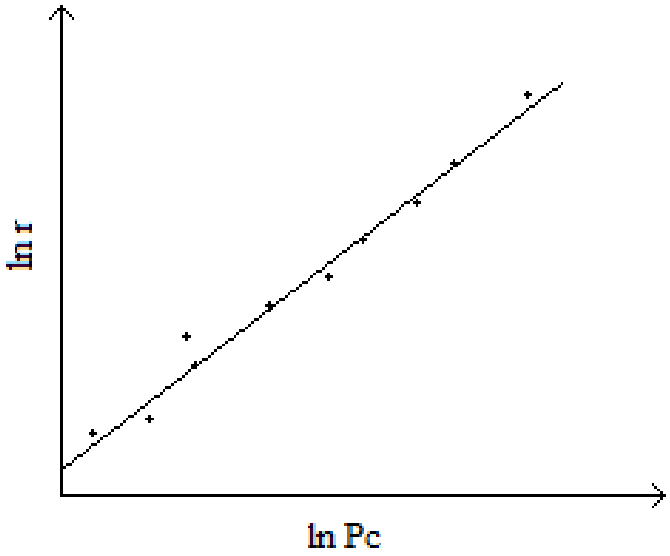

Fig. A.4.2.7.3.2: Plot of burning rate test data.
(John Beasley)

Figure A.4.2.7.3.2 shows how an equation is found relating burning rate to chamber pressure. The y-intercept is a, the burning rate coefficient. The slope of the line is n, the burning rate exponent. These two definitions result in the following relation.

$$\ln r = \ln a + n \ln P_c \qquad \text{(A.4.2.7.3.2)}$$

Removing the logarithms from Eq. (A.4.2.7.3.2) results in "St-Roberts Law," which is given in Eq. (A.4.2.7.3.3).

$$r = aP_c^{\,n} \qquad \text{(A.4.2.7.3.3)}$$

The next step is to choose an analytical method to determine performance. The simplest method is called the Steady Lumped Parameter Method. This method treats the entire combustion chamber as a single control volume. The goal is to find a single chamber pressure that is valid for the entire chamber. It also assumes that chamber pressures adjust instantly to changing conditions (quasi-steady state). The Unsteady Lumped Parameter method still treats the chamber

as a single control volume, but it allows for mass accumulation in the chamber. The third method, Ballistics with Spatial Pressure Variations divides the chamber into small 'ballistic elements.' This Ballistics approach allows for stagnation pressure losses along the chamber length and mass accumulation in the chamber. The Steady Lumped Parameter Method was implemented first in order to quickly replace the historical data we had been using with our own numerical data.

The following is a quick overview of the method. From continuity, the mass flow in equals the mass flow out. The mass flow rate into the control volume is a function of the burning rate, r, the burn surface area, A_b, and the propellant density, ρ_P.

$$\dot{m}_{in} = rA_b\rho_P \qquad \text{(A.4.2.7.3.4)}$$

The mass flow rate out of the chamber is a function of the chamber pressure, P_c, the throat area, A_t, and the characteristic velocity of the propellant, c^*.

$$\dot{m}_{out} = \frac{P_c A_t}{c^*} \qquad \text{(A.4.2.7.3.5)}$$

Setting Eq. (A.4.2.7.3.4) and Eq. (A.4.2.7.3.5) equal, substituting in Eq. (A.4.2.7.3.3), and rearranging results in the final formula for chamber pressure.

$$P_c = \left[\frac{a\rho_P A_b c^*}{A_t}\right]^{1/1-n} \qquad \text{(A.4.2.7.3.6)}$$

If the geometry of the engine and the propellant are known, the chamber pressure is found using Eq. (A.4.2.7.3.6). Conversely, the burn area can be determined based on a desired pressure history. Finally, the vacuum thrust is calculated based on the thrust coefficient, c_f, the chamber pressure, P_c, and the throat area, A_t.

$$F_{vac} = c_f P_c A_t \qquad \text{(A.4.2.7.3.7)}$$

For this analysis, we set an initial grain geometry. Then, the grain is burned back in small uniform steps. At each step, a new burn area is calculated. Next, the chamber pressure for each step is calculated using Eq. (A.4.2.7.3.6) and the vacuum thrust is found using Eq. (A.4.2.7.3.7). Then, the burning rate at each step is determined from Eq. (A.4.2.7.3.3). Finally, the mass flow rate is calculated using the Eq. A.4.2.7.3.5 and the time at each step is determined by using Eq. (A.4.2.7.3.8).

$$t = t_{i-1} + \frac{\Delta w}{r} \qquad \text{(A.4.2.7.3.8)}$$

where t is the time, t_{i-1} is the time at the previous step, Δw is the step size, and r is the burning rate.

Figure A.4.2.7.3.3 shows three initial geometries that were used to test the code, **Solid.m**. The resulting burn areas, chamber pressures, and mass flow rates are shown as functions of time in Fig. A.4.2.7.3.4, Fig. A.4.2.7.3.5, and Fig. A.4.2.7.3.6, respectively. Table A.4.2.7.3.1 shows the values for the other parameters.

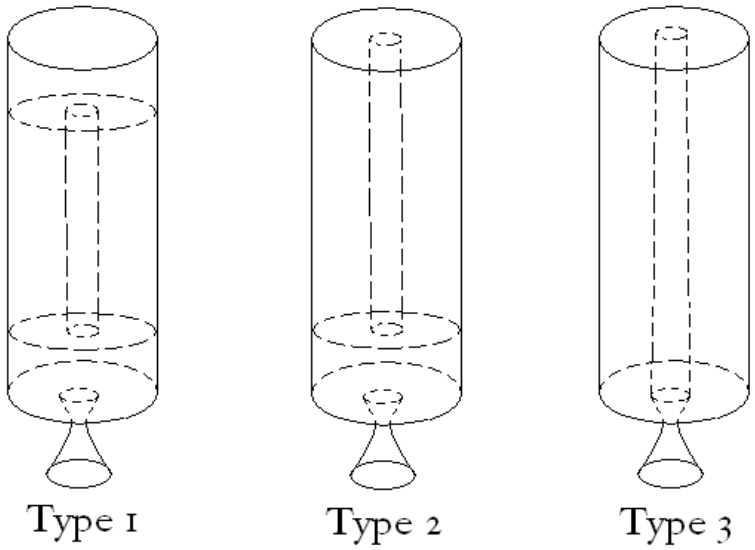

Figure A.4.2.7.3.3: Initial geometries used to test **Solid**.

(John Beasley)

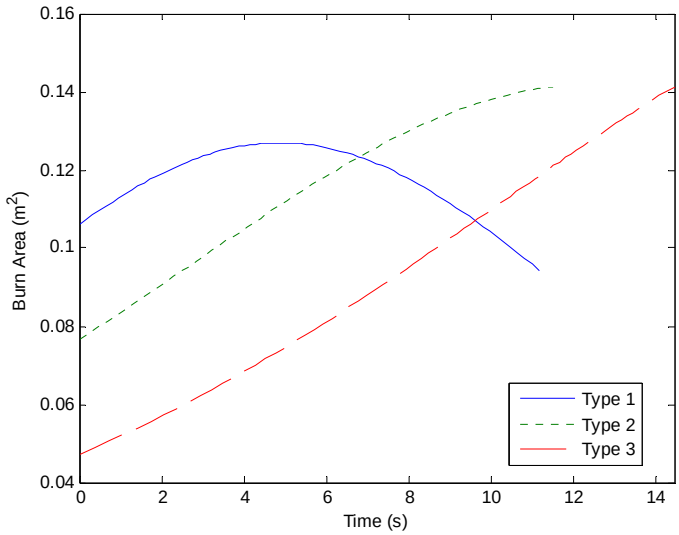

Figure A.4.2.7.3.4: Burn area profiles for test geometries.

(John Beasley)

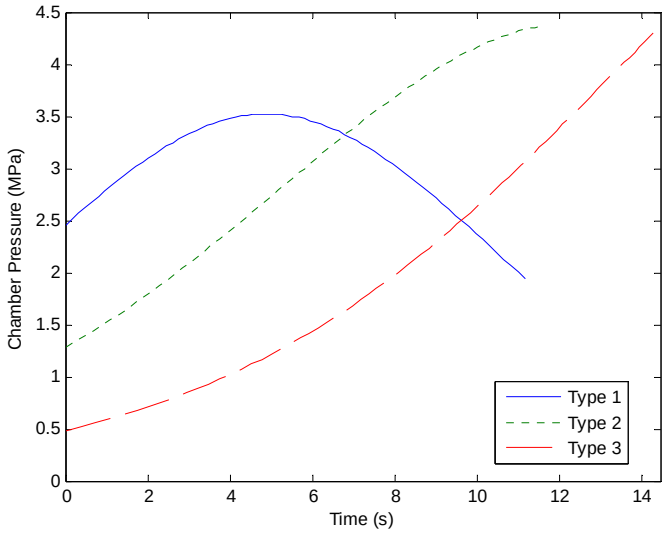

Figure A.4.2.7.3.5: Chamber pressure profiles for test geometries.

(John Beasley)

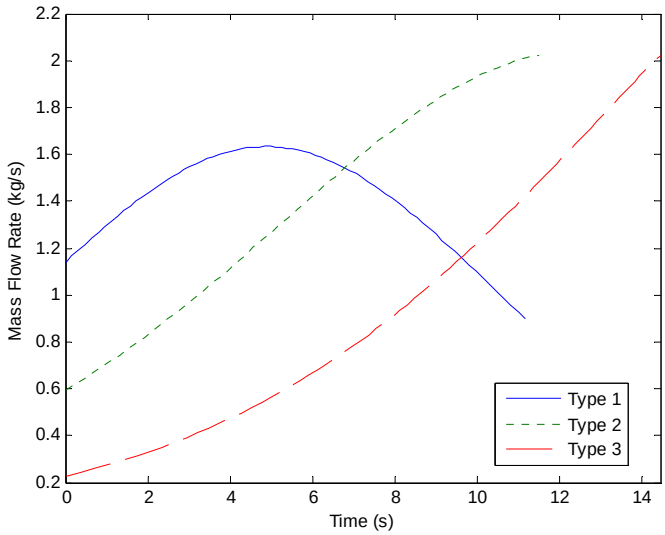

Figure A.4.2.7.3.6: Mass flow rate profiles for test geometries.

(John Beasley)

Table A.4.2.7.3.1 Parameters Used To Test **Solid**

Variable	Value	Units
a	0.0039	m/Mpa^0.5-s
n	0.5	--
A_t	7.07	Cm^2
ρ_P	1771.5139	Kg/m^3
c^*	1524	m/s
c_f	1.7	--
Δw	0.001	m

The next step would have been to integrate this code into the main design code. However, we decided to assume constant vacuum thrust to reduce the code runtime. At this point, work was stopped on solid rocket performance.

If more time is spent on this design project, there are several things that should be done in this area. First, some method that makes fewer assumptions than the Steady Lumped Parameter method should be implemented, such as the Ballistics with Spatial Pressure Variations method. Also, the geometry should be made self-optimizing. Currently, the geometry must be input manually and is static. To speed optimization, the code should be able to take parameters such as stage length, stage diameter, maximum chamber pressure, and desired initial thrust and modify the initial geometry to fit the required performance.

A.4.2.8 Testing

When it comes to testing our rocket engines we decided to try and design a launch vehicle which could be tested here at Purdue's Zucrow High Pressure Laboratories. After some research into the test labs at Purdue we as a team got a much better understanding of what we could accomplish here.

For testing rocket engines there are certain things that a facility must have in order to have a successful test. For example the test stand at Purdue's high pressure laboratories contains not only a 10,000 pound thrust stand, but also the capability to test liquid propellants such as hydrogen peroxide, liquid oxygen and liquid hydrocarbon. The facility currently has propellant tanks and tubing for these fuel and oxidizer types. This was also a factor in determining the propellant type for some of our designs. For example our hybrid rocket engines incorporate hydrogen peroxide (H_2O_2) as the oxidizer. Because of this Purdue would be a suitable candidate for testing. As for solid rocket engines there is no propellant that needs to be fed into the system because the test engine already has the solid propellant (fuel and oxidizer) built in. Because of this fact the only parameter that needs to be looked at for Purdue testing would be the test stands maximum thrust capability.

After researching Zucrow laboratories on Purdue's website and through various web articles and a visit to Zucrow we determined exactly how big of a rocket the facility could handle.[1] Some of the restrictions at Zucrow Laboratories are given below in Table A.4.2.8.1.

Table A.4.2.8.1: Purdue's Zucrow Laboratories facility restrictions.

Maximum Capability	Value	Units
Thrust	44,480	N
Chamber Pressure	4.137	MPa
Mass Flow Rate	6.803	kg/s

In the beginning of our design we tried to stay within these parameters. The first iteration of designs tried to keep these parameters as a limit to the performance of our rocket engine. On top

of this we also researched other facilities which could be used in case the rocket engine had a higher thrust than Purdue's facility could handle. When the final design was completed all of the rocket engines for all launch vehicles and all stages can be theoretically tested at Purdue given these parameters except for one. The stage one thrust for the 5 kilogram rocket has a design thrust of 75,073.2 Newtons. This is a higher thrust than the Zucrow laboratories can handle. For this engine an alternate test facility will be needed.

In order to find a test facility which could handle the amount of thrust that our largest final design rocket would need we had to look elsewhere other than Purdue. The best solution found was to test at Kelly Space and Technology's (KST) indoor rocket facility.[2] It is located in San Bernardino, CA. They have a thrust stand which can handle a maximum rocket thrust of 20,000 lbs which is approximately 88,960 Newtons. This is just in the range for the largest rocket that we would need to test. This facility already has propellant tanks and data acquisition systems which can be fitted to our specific needs. This facility would only be used to test our 5 kilogram stage one rocket engine. The maximum thrust for all of the launch vehicle engines is represented below in Table A.4.2.8.2 with a note on which facility it can be tested.

Table A.4.2.8.2: Maximum stage thrust and test facility.

Launch Vehicle	Max. Thrust	Units	Facility
5 kg			
Stage 1	75,073.2	N	KST
Stage 2	15,256.9	N	Purdue HPL
Stage 3	692.4	N	Purdue HPL
1 kg			
Stage 1	21,453.5	N	Purdue HPL
Stage 2	6,052.4	N	Purdue HPL
Stage 3	743.4	N	Purdue HPL
200 g			
Stage 1	34,045.3	N	Purdue HPL
Stage 2	8,782.6	N	Purdue HPL
Stage 3	625.0	N	Purdue HPL

As for the cost in order to perform a full rocket test at these facilities an accurate analysis was never completed. There were many factors to this but mainly because all of the sources that were

asked could not give an accurate price model. They stated that there were too many variables to be able to even ball park a figure. For this reason the cost of testing at Purdue and other facilities was not included in this stage of the design.

References

[1] Scott Meyer, private meeting at Zucrow Test Laboratories. February 8th, 2008. Test facility overview and private tour of the large rocket test stand.

[2] Kelly Space and Technology. Jet and Rocket Engine Test Site (JRETS) URL: http://www.kellyspace.com/ [last updated Jan. 31st 2008].

A.4.3 Closing Comments

The previous pages in the propulsion group's section give an in-depth look at all the work conducted by our group throughout the semester. The propulsion system of our launch vehicle is a very vital and complicated part. Our team uses the best data from our research in order to use the best and most cost effective propulsion system.

Throughout the semester, our group went through very lengthy analysis of many different aspects of propulsion systems. Some of the areas looked at throughout the research included propellant types, injectors, nozzles, attitude control systems, and engine performance. Through the research gathered, our group developed a set of different propulsion options that were then used to optimize the vehicle. The optimization process led us to the best possible cost-effective propulsion system that will enable our launch vehicle to carry each specified payload into low Earth orbit.

A.4.4 User's Guides for Propulsion Codes

User's Guide for *prop_code_1.m*

Written by Nicole Wilcox, Stephen Bluestone, and Alan Schwing
Assistance from John Tsohas, Dana Lattibeaudiere, and John Beasley

Description:
This code uses information from the NASA Chemical Equilibrium with Applications program to set up vectors that will feed into three_stages.m for calculating optimum launch vehicle staging, propellant mass, and cost. The code was integrated into the Model Analysis codes to optimize fuel and structural selection.

Assumptions:

- Thrust is assumed constant
- Isp is assumed vacuum for all three stages with balloon launch
- Mass flow rate is constant
- Area ratio based on historical data
- Isp is assumed sea level for first stage ground launch
- No throttle

Important Notes:

The NASA Chemical Equilibrium with Applications code was used to find all rocket performance parameters. These parameters are designed for a set expansion ratio and chamber pressure.

The variables of vector form are in order of stage. For instance position 1 of vector x refers to the value correlating with stage one.

Input Section:

The call line of the function is:
function [inert_mass, prop_mass, volume_ox, volume_fuel, cost_stage,cost_total, mass_fuel, mass_ox, delta_v_per, rho_ox, rho_f, O_F, e, gam, c_star, cf, Ispv, Isp, Pc_Pe, a, M, Tc, Pc] = prop_code_1(delta_v,launch_type,num_stage,prop_stage,mass_payload,f_inert,P1,P2,mass_avionics)

Input Section:

Variable Name	Description
delta_v	Total delta v needed for orbit insertion (scalar) [m/s]
launch_type	Launch type (ground, balloon, aircraft) (scalar)
num_stage	Number of stages (scalar)
prop_stage	Propellant to be used in each stage (vector)
mass_payload	Mass of the payload (scalar) [kg]
f_inert	Inert mass fraction (vector)
P1	Percentage of delta v for first stage (scalar)
P2	Percentage of delta v for second stage (scalar)
mass_avionics	Mass of avionics equipment in each stage (vector) [kg]

Output Section:

Variable Name	Description
inert_mass	Inert mass of each stage (vector) [kg]
prop_mass	Mass of propellant each stage (vector) [kg]
volume_ox	Volume of oxidizer in each stage (vector) [m^3]
volume_fuel	Volume of fuel in each stage (vector) [m^3]
cost_stage	The cost of propellant for each stage (vector) [$]
cost_total	Total cost of propellant (scalar) [$]
mass_fuel	Mass of fuel in each stage (vector) [kg]
mass_ox	Mass of oxidizer in each stage (vector) [kg]
delta_v_per	Delta v acquired per stage (vector) [m/s]
rho_ox	Density of oxidizer in each stage (vector) [kg/m^3]
rho_f	Density of fuel in each stage (vector) [kg/m^3]
O_F	Oxidizer to fuel ratio in each stage (vector)
e	Expansion ratio of each stage (vector)
gam	Specific ratio for each stage (vector)
c_star	Characteristic velocity for each stage (vector) [m/s]
cf	Coefficient of thrust for each stage (vector)
Ispv	Vacuum specific impulse for each stage (vector) [s]
Isp	Sea level specific impulse for each stage (vector) [s]
Pc_Pe	Chamber to exit pressure ratio for each stage (vector)
a	Speed of sound at exit for each stage (vector) [m/s]
M	Exit mach number at exit for each stage (vector) [m/s]
Tc	Chamber temperature for each stage (vector) [K]
Pc	Chamber pressure for each stage (vector) [Pa]

Flow Chart:

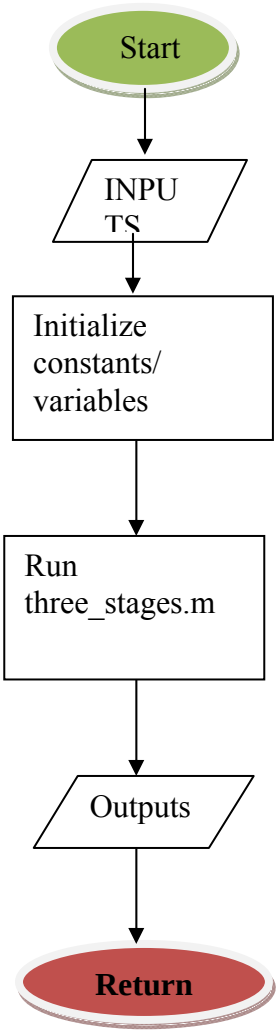
Start
INPU
TS
Initialize constants/ variables
Run three_stages.m
Outputs
Return

User's Guide for *three_stages.m*

Written by Stephen Bluestone and Nicole Wilcox
Assistance from Alan Schwing, John Tsohas, Dana Lattibeaudiere
Revision 2.0 - 31 Jan 08

Description:

This code is designed to find the mass of propellant, propellant volume, propellant cost, and inert mass based off inputs of propellant performance and selected inert mass fractions imported from *prop_code_1.m*. Output from this code would be used in Model Analysis to optimize the size of the launch vehicle.

Assumptions:

- The input of specific impulse, oxidizer-to-fuel ratio, and ΔV for each stage are provided
- Propellants are at constant density

Important Notes:

It was found early on in the design of this code that if the Mass Ratio exceeded one over the inert mass fraction the code would run into difficulties when calculating the mass of propellant. Therefore several lines of logic were placed in the code to prevent calculation if this situation occurred. The code will skip to the next iteration from Model Analysis if this happened.

Additional logic was added at the end of *three_stages.m* to catch any negative answers that are calculated. Occasionally negative propellant masses would appear so a catch was placed to set all output values to zero if this occurred.

The division of ΔV between the three stages is imported to this code as a two part vector for the first two stages. The percentage of ΔV for the third stage is calculated internally by subtracting the percentage of the first two stages from one.

All parameters are in the form of arrays.

Input Section:

The call line of the function is:

```
[mass_tot_1,mass_tot_2,mass_tot_3,mass_prop_1,mass_prop_2,...
   mass_prop_3,cost_total,cost_1,cost_2,cost_3,volume_ox_3,volume_ox_2,...
   volume_ox_1,volume_f_3,volume_f_2,volume_f_1,dv_1,dv_2,dv_3,...
   mass_fuel_1, mass_fuel_2, mass_fuel_3, mass_ox_1, mass_ox_2,
mass_ox_3,mass_total,mass_inert_1,mass_inert_2,mass_inert_3]=Three_stages(Isp,...
   dv,f_inert,mpl,O_F,cost_o,cost_f,avionics,rho_ox,rho_f,P1,P2)
```

All of the variables that are passed into the function are described below:

Variable Name	**Description**
Isp	Specific Impulse (vector) [s]
dv	ΔV (scalar) [m/s]
f_inert	Inert Mass Fraction (vector) [%]
mpl	Payload Mass (scalar) [kg]
O_F	Oxidizer-to-Fuel Ratio (vector)
cost_o	Cost of Oxidizer (vector) [$]
cost_f	Cost of Fuel (vector) [$]
avionics	Avionics Mass (vector) [kg]
rho_ox	Density of Oxidizer (vector) [kg/m^3]
rho_f	Density of Fuel (vector) [kg/m^3]
P1	Percentage of ΔV for 1st Stage (scalar) [%]
P2	Percentage of ΔV for 2nd Stage (scalar) [%]

Output Section:

All variables that come out of the code are described below:

Variable Name	**Description**
mass_tot_1	Total Mass of 1st Stage (scalar) [kg]
mass_tot_2	Total Mass of 2nd Stage (scalar) [kg]
mass_tot_3	Total Mass of 3rd Stage (scalar) [kg]
mass_prop_1	Propellant Mass for 1st Stage (scalar) [kg]
mass_prop_2	Propellant Mass for 2nd Stage (scalar) [kg]
mass_prop_3	Propellant Mass for 3rd Stage (scalar) [kg]
cost_1	Propellant Cost for 1st Stage (scalar) [$]
cost_2	Propellant Cost for 2nd Stage (scalar) [$]
cost_3	Propellant Cost for 3rd Stage (scalar) [$]
vol_ox_1	Oxidizer Volume for 1st Stage (scalar) [m^3]
vol_ox_2	Oxidizer Volume for 2nd Stage (scalar) [m^3]
vol_ox_3	Oxidizer Volume for 3rd Stage (scalar) [m^3]
vol_f_1	Fuel Volume for 1st Stage (scalar) [m^3]
vol_f_2	Fuel Volume for 2nd Stage (scalar) [m^3]
vol_f_3	Fuel Volume for 3rd Stage (scalar) [m^3]
dv_1	ΔV for 1st Stage (scalar) [m/s]

dv_2	ΔV for 2nd Stage (scalar) [m/s]
dv_3	ΔV for 3rd Stage (scalar) [m/s]
mass_fuel_1	Fuel Mass for 1st Stage (scalar) [kg]
mass_fuel_2	Fuel Mass for 2nd Stage (scalar) [kg]
mass_fuel_3	Fuel Mass for 3rd Stage (scalar) [kg]
mass_ox_1	Oxidizer Mass for 1st Stage (scalar) [kg]
mass_ox_2	Oxidizer Mass for 2nd Stage (scalar) [kg]
mass_ox_3	Oxidizer Mass for 3rd Stage (scalar) [kg]
mass_total	Total Mass of Launch Vehicle (scalar) [kg]
mass_inert_1	Inert Mass for 1st Stage (scalar) [kg]
mass_inert_2	Inert Mass for 2nd Stage (scalar) [kg]
mass_inert_3	Inert Mass for 3rd Stage (scalar) [kg]

Flow Chart:

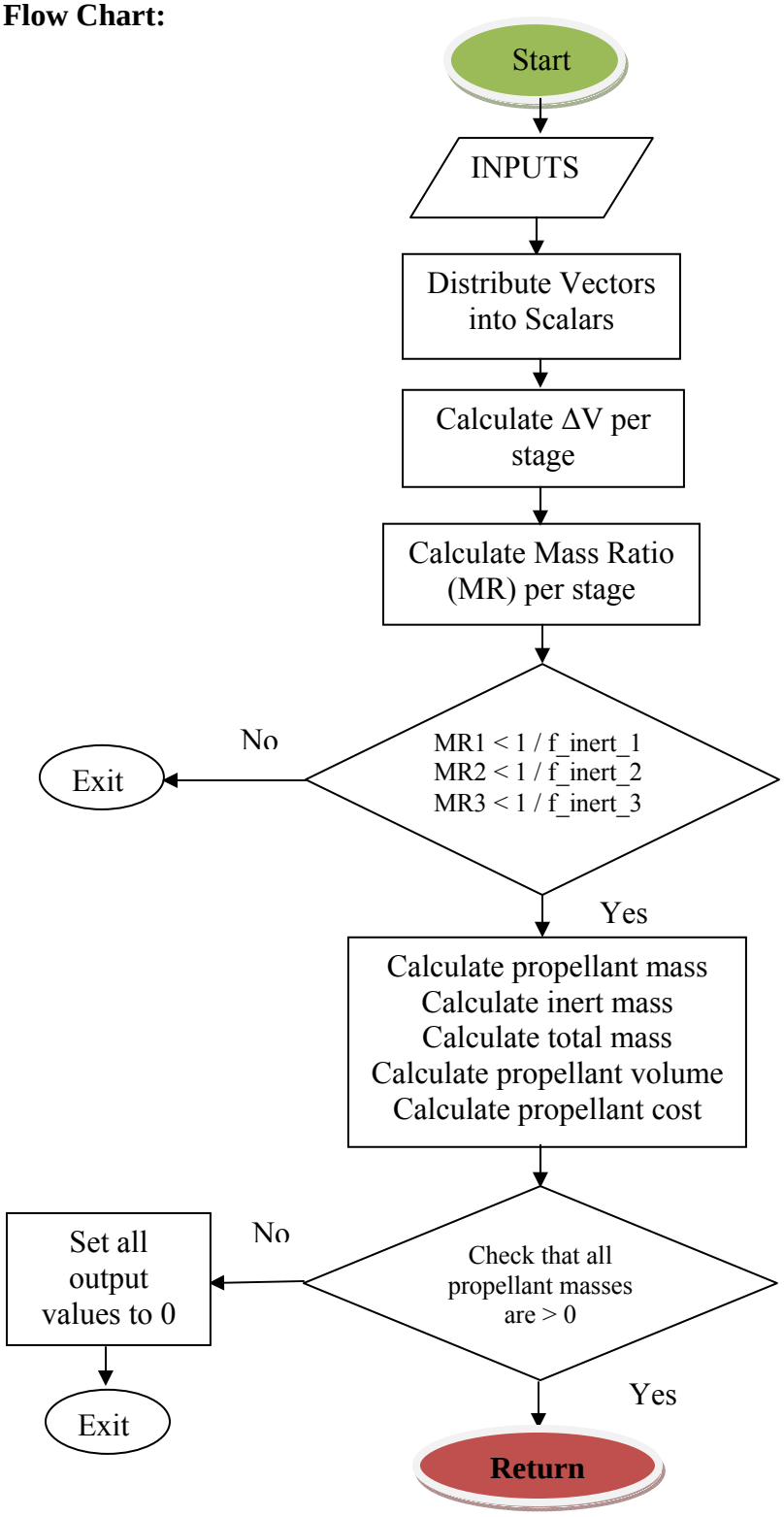
Start
INPUTS
Distribute Vectors into Scalars
Calculate ΔV per stage
Calculate Mass Ratio (MR) per stage
MR1 < 1 / f_inert_1
MR2 < 1 / f_inert_2
MR3 < 1 / f_inert_3
No
Exit
Yes
Calculate propellant mass
Calculate inert mass
Calculate total mass
Calculate propellant volume
Calculate propellant cost
Check that all propellant masses are > 0
No
Set all output values to 0
Exit
Yes
Return

User's Guide for *pressurant.m*

Written by Nicole Wilcox
Assistance from Stephen Bluestone

Description:
This code calculates the amount of pressurant to be used for the pressure-fed propellant feed system.

Assumptions:

- Volume of pressurant tank is assumed negligible
- Isentropic flow assumed for expansion

Important Notes:

The NASA Chemical Equilibrium with Applications code was used to find all rocket performance parameters. These parameters are designed for a set expansion ratio and chamber pressure.

The variables of vector form are in order of stage. For instance position 1 of vector x refers to the value correlating with stage one.

Input Section:

The call line of the function is:
function [cost_total, volume_pressurant, P_press, m_press, cost_stage] = pressurant(volume_ox, volume_fuel, cost_total, stages, propellant_type, cost_stage);

Input Section:

Variable Name	Description
volume_ox	Volume of oxidizer for each stage (vector) [m^3]
volume_fuel	Volume of fuel for each stage (vector) [m^3]
cost_total	Total cost of propellant (scalar) [$]
stages	Stages with pressurant (vector)
propellant_type	Type of propellant in each stage (vector)
cost_stage	Cost per stage (vector) [$]

Output Section:

Variable Name	Description
cost_total	Cost of propellant and pressurant total (scalar) [$]
volume_pressurant	Volume of pressurant for each stage (vector) [m^3]
P_press	Pressure of pressurant for each stage (vector) [Pa]
m_press	Mass of pressurant for each stage (vector) [kg]
cost_stage	Cost of propellant and pressurant for each stage (vector) [$]

Flow Chart:

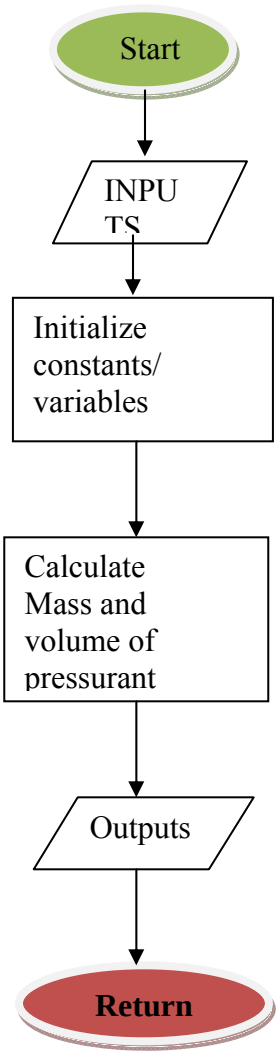

User's Guide for *Hybrid.m*

Written by John Beasley

Description:

The script **Hybrid.m,** along with functions **Hybrid_Area.m** and **cstar_lookup.m,** produces time histories for chamber pressure, thrust, burn area, and port area based on user inputs.

User Inputs:

The following values are put into the input section of the script.

Variable Name	Description
port_diameter	port diameter (m)
outer_radius	grain outer radius (m)
inner_radius	radius of central port (m)
port_offset	diagonal distance between center of main ports (m)
length	grain length (m)
dw	burn step size (m)
tolerance	tolerance for iteration
mdot_ox	oxidizer mass flow rate (kg/s)
rho_f	fuel density (kg/m^3)
A_t	throat area (m^2)
gam	ratio of specific heats
e	expansion ratio
cone_angle	nozzle cone angle (deg)
g	gravity (m/s^2)

cstar_lookup.m Inputs:

row is a vector that contains n-values for chamber pressure. column is a vector that contains m-values for mixture ratio. table is a n-by-m matrix that contains the characteristic velocity taken from the NASA CEA code. Element i,j uses the output for the i-th chamber pressure and the j-th mixture ratio.

Output:

The script generates plots vs. time for chamber pressure, thrust, burn area, burn rate, mass flow rate. All other values used in the code are saved in the workspace in vector format.

User's Guide for *Solid.m*

Written by John Beasley

Description:

The script **Solid.m,** and function **solid_area.m,** produces time histories for chamber pressure, burn area, burn rate, mass flow rate, and vacuum specific impulse based on user inputs.

User Inputs:

The following values are put into the input section of the script.

Variable Name	Description
a	burn rate coefficient (cm/s-MPa^n)
rho_p	propellant density (kg/m^3)
n	burn rate exponent
c_star	characteristic velocity (m/s)
A_t	throat area (m^2)
g	gravity (m/s^2)
t_0	initial time (s)
c_f	nozzle efficiency factor
Ri	grain inner radius (m)
Ro	grain outer radius (m)
L	grain length (m)
type	burn type
dw	burn step size (m)

Output:

The script generates plots vs. time for chamber pressure, burn area, burn rate, mass flow rate.

All other values used in the code are saved in the workspace in vector format.